

Real-time Neural Force Estimation and Model-free Control of Interventional Catheters

Hamidreza Khodashenas

A Thesis

in

The Department

of

Mechanical, Industrial, Aerospace Engineering

Presented in Partial Fulfillment of the Requirements

for the Degree of

Master of Applied Science (Mechanical Engineering) at

Concordia University

Montréal, Québec, Canada

November 2022

© Hamidreza Khodashenas, 2022

CONCORDIA UNIVERSITY

School of Graduate Studies

This is to certify that the thesis prepared

By: **Hamidreza Khodashenas**

Entitled: **Real-time Neural Force Estimation and Model-free Control of Interventional Catheters**

and submitted in partial fulfillment of the requirements for the degree of

Master of Applied Science (Mechanical Engineering)

complies with the regulations of this University and meets the accepted standards with respect to originality and quality.

Signed by the Final Examining Committee:

Dr. Behrooz Yousefzadeh Chair

Dr. Behrooz Yousefzadeh Examiner

Dr. Ion Stiharu Examiner

Dr. Javad Dargahi Supervisor

Approved by

Dr.Martin Pugh, Chair
Department of Mechanical, Industrial, Aerospace Engineering

Nov.23, 2022

Dr.Mourad Debbabi, Dean
Faculty of Engineering and Computer Science

Abstract

Real-time Neural Force Estimation and Model-free Control of Interventional Catheters

Hamidreza Khodashenas

One of the most common forms of heart arrhythmia is atrial fibrillation, a disorder caused by the uncoordinated electrical distribution of heart muscle. Catheter ablation is an effective treatment of choice for this heart disorder that destroys the arrhythmogenic spots in the heart muscle to recover the normal beating of the heart. To perform this minimally invasive surgery, the surgeon inserts a flexible and steerable wire-like tool, called ablation catheter into the cardiovascular system of the body. After reaching the target spot inside the heart chamber, the surgeon or robotic system pushes the catheter's tip against the heart tissue. Afterward, the heat generated by the embedded electrode at the tip of the catheter burns the target spot. A properly controlled catheter-tissue contact force (CF) results not only in a safer procedure, but also considerably increases the success of treatment. To this end, the main motivation of the present thesis is to propose an accurate learning-based CF estimator and then use it in a control loop. This research is a proof of concept for estimating and controlling the CF. An experimental setup was designed in an attempt to mimic the ablation surgery. Firstly, a vision-based method using machine learning model is proposed in order to estimate the CF without using a sensor at the tip of the catheter. This model requires the image of bending section of catheter to output the CF. The real image should come from the X-ray machine in the operating room but to simulate the X-ray imaging system, in this research, a camera was implemented. This real-time and sensor-free technique provides acceptable accuracy when estimating the CF of standard catheters. A catheter manipulator mechanism is implemented to control the CF at the desired value. The feedback element of the control loop is the mentioned vision-based force estimator. In addition, an adaptive imaging system including a robotic arm and camera is implemented to track the catheter for force control.

Acknowledgments

This thesis is the result of two years of effort in the most memorable period of my life. Today, I am extremely glad to contribute to the medical technology area to help people in the world for one of the considerable clinical needs. I also could not have undertaken this achievement without the support of my loved ones. My study started in the Winter of 2020 as an international student in Canada and this journey has had many ups and downs. When I started my study, all Iranian students were shocked by the tragedy of the PS752 flight, and I would like to express my deepest sympathies to the family of victims of this flight. We will never forget the victims. Peace be upon their soul.

I would like to thank my supervisor, Prof. Javad Dargahi for his support during my study and for giving me the opportunity to work in a great research laboratory.

Words cannot express my gratitude to my family for their love, support, and motivation. My father, Mojtaba who I learned the real meaning of “never give up” from him, and my mother, Nahid teaches me generosity and love in life. My brother, Alireza, for his kindness and support in all moments.

This endeavor would not have been possible without the generous support of my colleagues and friends. I would like to thank, Dr. Amir Hooshidar, Dr. Naghmeh Bandari, Hamid Nourani, Amir Sayadi, Salar Taki, Shahideh Roshan, Saman Namvar, Nikta Tabesh, Sevin Samadi, Mohammad Jolaei, and Reza Khoshbakht.

Finally, a special thanks to the faculty and staff of Concordia University and Gina Cody School of Engineering and Computer Science for their support during my study. I am also thankful to all members of the surgical innovation program at McGill University.

To the loves of my life:

My father, my mother, and my brother

Contents

List of Figures	ix
List of Tables	xi
Nomenclatures	xii
1 Introduction	1
1.1 Background	1
1.1.1 Cardiovascular Diseases	1
1.1.2 Treatments	2
1.1.3 Robotic-assisted surgery	3
1.1.4 Robotic systems for cardiac ablation surgery	7
1.1.5 Ablation lesion’s formation and importance of contact force	9
1.1.6 Problem definition based on the clinical need	10
1.2 Literature Review	12
1.2.1 Sensor technologies	13
1.2.2 Mechanical model methods	16
1.2.3 Learning-based estimation	18
1.3 Objectives	22
1.4 Publications	23
1.5 Thesis layout and contributions	23

2	Data Collection and Experimental Setup Design	26
2.1	Introduction	26
2.2	Review of available setups	27
2.3	Uni-planar imaging setup	29
2.3.1	Automation algorithm	32
2.3.2	Vision system	33
2.3.3	Data	35
2.4	Catheter manipulator mechanism	37
2.5	Summary	38
3	A Vision-based Method For Estimating Contact Forces In Intracardiac Catheters	39
3.1	Introduction	40
3.2	Experimental setup and procedure	41
3.2.1	Experimental setup design	42
3.2.2	Data Collection	42
3.3	Methodology	45
3.3.1	Feature extraction	45
3.3.2	Machine Learning Models	45
3.4	Results and Discussion	49
3.5	Conclusions	51
4	Force control on intracardiac catheters through adaptive monoplanar imaging and neural force estimation	52
4.1	Introduction	53
4.1.1	Background	53
4.1.2	Related studies	55
4.1.3	Contributions	57
4.2	Methodology	57
4.2.1	Force control framework	58
4.2.2	Neural force estimation	58

4.2.3	Controller design	60
4.2.4	Experimental setup	60
4.3	Validation studies	64
4.3.1	CF estimator evaluation	64
4.3.2	Static force control	65
4.3.3	Dynamic force control	66
4.4	Conclusion	67
5	Conclusion and Future Works	69
5.1	Conclusions	69
5.2	Future Works	71
	Bibliography	72

List of Figures

Figure 1.1	The heart’s electrical signal distribution. The electrical potential starts from the sinoatrial(SA) node and travels through the heart muscle. Due to arrhythmogenic spots of heart tissue, the erratic impulses occur.	2
Figure 1.2	Radio-frequency ablation treatment for atrial fibrillation. An ablation catheter is inserted into the cardiovascular system of the body from the femoral vein of the leg to access the target spots inside the heart chamber	4
Figure 1.3	The <i>Cartounivu</i> ® mapping system showing the catheter and abnormal spots of heart. (Biosense Webster Inc., California, USA)	5
Figure 1.4	Da Vinci robotic system(Intuitive Inc., California, USA)	6
Figure 1.5	Ion platform(Intuitive Inc., California, USA)	6
Figure 1.6	Mako robotic arm system (Stryker Inc., Michigan, USA)	7
Figure 1.7	Ablation Catheter and steerable sheath- (a): Standard ablation catheter’s handle(Boston Scientific Blazer II XP) - (b): Different sections of the shaft of ablation catheter - (C): Steerable ablation sheath(Boston Scientific, USA)	11
Figure 1.8	Commercially available sensing technologies of ablation catheters- (a):TactiCath™ contact force ablation catheter(Abbott Laboratories, Abbott Park, Illinois, USA) - (b):Thermocool@catheter(Biosense Webster Inc., California, USA) - (c):Directsense™ technology (Boston Scientific Corporation, Marlborough, Massachusetts, USA)	15
Figure 1.9	Machine learning procedure	20
Figure 2.1	Fluoroscopy system Allura Xper FD10 - Philips, Netherlands	30
Figure 2.2	Uni-planar experimental setup	31

Figure 2.3	Software and hardware interaction of the setup for data acquisition	33
Figure 2.4	Chessboard calibration images	34
Figure 2.5	(a), (b), and (c) are Aruco markers in different orientation of camera - (d) is a view of the marker beside the catheter's distal shaft	35
Figure 2.6	Images from the uni-planar dataset	36
Figure 2.7	Force samples of the uni-planar setup	37
Figure 2.8	3-DoF Catheter manipulator mechanism capable of insertion, rotation, and knob actuation	38
Figure 3.1	Experimental Setup	43
Figure 3.2	Software and hardware interaction	44
Figure 3.3	Features Extraction	46
Figure 3.4	The performance of the SVR for approximating the forces in both x and y direction.	50
Figure 3.5	This plot shows the performance of the designed ANN in estimating the forces in x and y direction.	50
Figure 4.1	Ablation catheters inside the heart chamber	54
Figure 4.2	Overview of the system	57
Figure 4.3	Proposed neural CF estimator	58
Figure 4.4	controller	61
Figure 4.5	Experimental setup	62
Figure 4.6	Model performance analysis - (a) Training loss diagram for validation and training set, (b) Correlation of the reference values from test set and the estimation of the model, (c) Error distribution, (d) Comparison of all actual and predicted CFs.	65
Figure 4.7	Step response analysis	66
Figure 4.8	Validation tests - (a) Static force input, (b) 0.5 Hz sinusoidal force input, (c) 1Hz sinusoidal force input	67

List of Tables

Table 1.1 Commercially available robotic-assisted ablation surgery systems 8

Table 3.1 The performance of multiple modeling methods with different configurations. 48

Nomenclatures

Abbreviation

CVD

AF

AV node

SA node

MIS

RF

EAM

FDA

DOF

CF

DAQ

SVM

ANN

IMU

SVR

DL

MAE

MSE

ML

DNN

RMS

EM

BN

ReLU

English Symbols

W

b

f

K_p

K_d

x

y

z

Cardiovascular Disease

Atrial Fibrillation

Atrioventricular node

Sinoatrial node

Minimally Invasive Surgery

Radio Frequency

Electroanatomical Mapping

Food and Drug Administration

Degrees of Freedom

Contact Force

Data Acquisition

Support Vector Machine

Artificial Neural Network

Inertial Measurement Unit

Support Vector Regression

Deep Learning

Mean Absolute Error

Mean Squared Error

Machine Learning

Deep Neural Network

Root Mean Square

Electromagnetic

Batch Normalization

Rectified Linear Unit

Weight

Bias

Actual Force

Proportional Gain

Derivative Gain

x-component of the force

y-component of the force

z-component of the force

Chapter 1

Introduction

1.1 Background

1.1.1 Cardiovascular Diseases

Cardiovascular Diseases(CVDs) as one of the main reasons of worldwide mortality are affecting at least 17 million people annually [1]. According to the report of the Center for Disease Control and Prevention of the United States(CDC), every 36 seconds, one person dies in the United States due to cardiovascular failures [2]. Among cardiac disorders, atrial fibrillation (AF) is the most common type caused by faulty electrical signal distribution within the heart. A recent report from the American Heart Association estimates that the prevalence of AF in the US will reach 13.1 million in 2023, and 17.9 million in the EU by 2060 [3].

Electric pulses through the heart muscles regulate the heart's pumping functionality or cardiac cycle. As shown in Figure.1.1, the sinus node located in the right atrium of the heart functions as a natural pacemaker specialized to generate signals to be transferred into the cardiac electrical pathway. The atrioventricular node (AV node) in the right atrium slows down the generated action potential before it reaches the heart's electrical network to ensure that contractions perform at the normal time [4]. In the event of failure of this distribution network, a heart abnormality may occur.

As a result of erratic electrical pulses, AF is treated as an abnormality of the heart beating. The

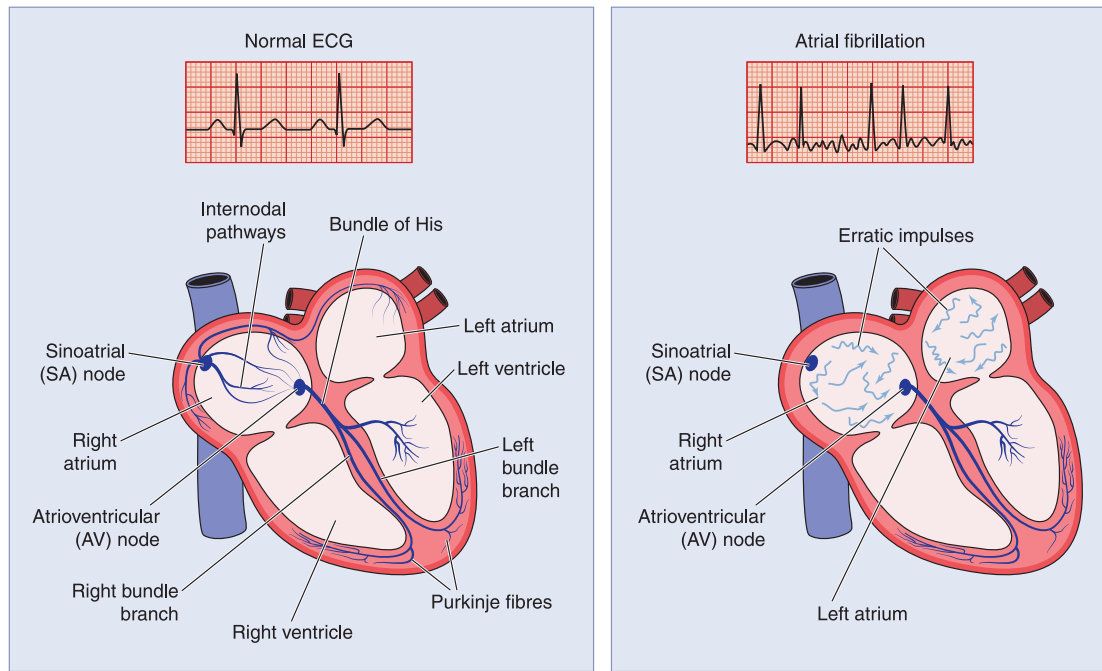


Figure 1.1: The heart's electrical signal distribution. The electrical potential starts from the sinoatrial(SA) node and travels through the heart muscle. Due to arrhythmogenic spots of heart tissue, the erratic impulses occur.

risk of stroke and related cardiac problems is high in patients with AF, which is justified as a 21st-century global epidemic [5, 6]. Figure.1.1 illustrates some arrhythmogenic spots inside of the heart causing the irregularity in heart beating. Consequently, the impaired signals are transmitted through the electricity network since these spots block normal transmission of electrical signals [7].

1.1.2 Treatments

After identifying the reason for heart arrhythmia, proper treatment should be taken. To manage AF, three treatment strategies are considered including stroke prevention, sinus rhythm control, and heart rate control during AF. In general, The corresponding treatment choices for all of these strategies fall into two methods: Pharmacological and Non-pharmacological therapy[8].

In spite of the fact that the first-line pharmacological treatment for AF is anti-arrhythmic and rate-control drugs, non-pharmacological treatments, such as ablation therapy, showed superior results in terms of recurrence of AF[8]. In this regard, Wazni *et al.*[9] conducted a randomized clinical

trial of 70 patients who suffered from AF and showed that ablation therapy works better than drugs in treating AF. In this study, among the patients who received anti-arrhythmic drugs, 63% had recurrences of AF, whereas just 13% of those who received ablation had recurrences.

Minimally invasive surgery(MIS) due to its benefits such as lower hospitalization period, lower blood loss, and infection is the procedure of the choice for many surgeons[10]. Ablation therapy is an MIS for destroying (ablating) the target spots of the heart muscle causing electrical disturbances. It involves inserting a flexible wire-like tube into the cardiovascular system of the body through a small skin incision in order to reach the locations of the arrhythmia inside the heart[11]. This tube is known as an ablation catheter, which transfers energy to the area of interest for ablation[12]. The ablation catheter's tip is equipped with an electrode that is connected to a radio frequency (RF) generator device outside of the patient's body, as demonstrated in Figure.1.2, RF employs electric current in a specific frequency range to heat tissue surrounding the catheter's electrode and as the result, the heated region can be destroyed[12].

As part of the heart ablation procedure, the surgeon inserts a catheter into a blood vessel, usually a femoral vein, and steers it to the heart. An actuating knob on a tendon-driven catheter can be rotated from outside the body of the patient in order to control the tip's location[13]. To ablate the tissue, the surgeon applies the adequate tissue-tip force known as contact force and activates the RF generator for a determined time. To ensure that all arrhythmic areas in the heart are ablated, this procedure should be repeated for all detected spots[14].

1.1.3 Robotic-assisted surgery

The ablation surgery performs under a X-ray imaging system. The fluoroscopy imaging system captures real-time images from the patient that allows the surgeon to track the catheter[15]. In addition, an electroanatomical mapping system (EAM) displays heart arrhythmia spots in a color-coded representation using 3D reconstruction techniques as shown in Figure.1.3 [16].

While fluoroscopy systems are advantageous in catheterization procedures, x-ray exposure may lead to some health risks for both patients and physician[17]. Ablation surgery takes about four hours from catheter insertion to ablation therapy termination, with an hourly risk for cancer and

CARDIAC ABLATION FOR ATRIAL FIBRILLATION

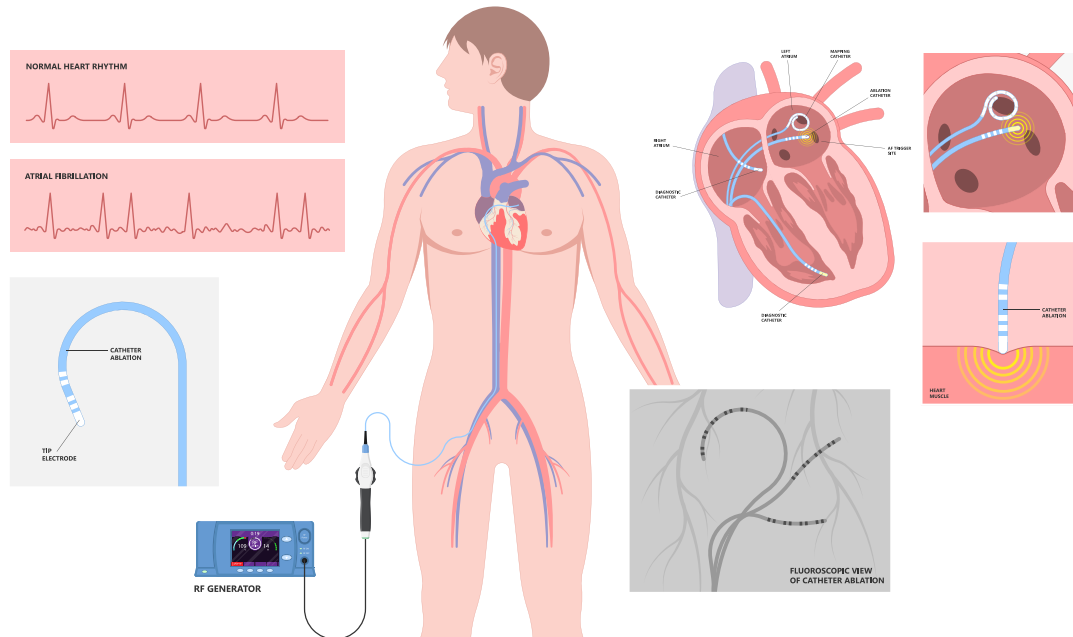


Figure 1.2: Radio-frequency ablation treatment for atrial fibrillation. An ablation catheter is inserted into the cardiovascular system of the body from the femoral vein of the leg to access the target spots inside the heart chamber

genetic defects for all people under the exposure[18]. To overcome these health risks for the surgeon and patient, robotic-assisted surgery has been implemented[19]. In recent years due to the considerable advantages of robotic systems in surgery, these systems have been used in a variety of operations such as minimally invasive cardiac, gynecology, orthopedic, and laparoscopy[20, 21, 22]. In comparison with open surgery, minimally invasive robotic surgeries offer some remarkable benefits consisting of:

- Low risk of infection and blood loss due to small incision size
- Faster patient recovery resulting in shorter hospitalization
- Greater vision for the surgeon because of enhanced visualization systems
- Enhanced precision of the surgical procedure
- The possibility of performing live broadcasting of surgery with more expert surgeons[23]

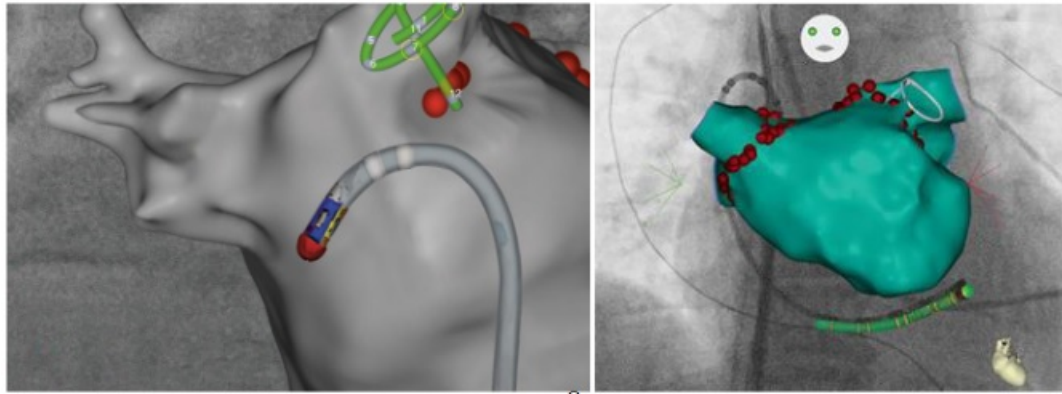


Figure 1.3: The *Cartounivu*® mapping system showing the catheter and abnormal spots of heart. (Biosense Webster Inc., California, USA)

- The capability of telerobotic surgeries

Following is a brief review of three well-known robotic systems for different types of surgeries:

Da Vinci robotic system by Intuitive Surgical Inc., known as the most common system in medical applications. The FDA (Food and Drug Administration) approved this system in 2000, which consists of a surgeon's console and robotic arms. The surgeon can move the robotic arms with haptic joysticks in the console to perform the surgery. The console is equipped with a screen to provide a clear view from the camera of the robot for the surgeon. Furthermore, depending on the type of procedure, a variety of surgical tools such as scissor, scalpel, and grasper could be attached to the end effector of robotic arms to be used by the surgeon[24]. It is also noticeable that, in an attempt to train surgeons, the system is capable of simulating surgical procedures.

Ion by Intuitive Surgical Inc. is another newly approved system that allows surgeons to perform minimally invasive lung biopsy surgery. This system is equipped with an actuatable ultra-thin catheter that goes into the airways and reaches the target area inside the lung. The flexible catheter helps surgeons to reach the spots in the lung that are not accessible easily[25].

In orthopedic operations, *MAKO* by Stryker Inc. is a robotic platform that can assist surgeons with knee and hip procedures. By using CT images of the patient, this system can pre-plan the surgery in such a way that the implants are positioned accurately. Before starting the surgery, the surgeon can review the procedure for some modifications and finally during the surgery the robotic arm just allows the physician to perform the surgery in the defined boundaries[26]. As the



Figure 1.4: Da Vinci robotic system(Intuitive Inc., California, USA)



Figure 1.5: Ion platform(Intuitive Inc., California, USA)



Figure 1.6: Mako robotic arm system (Stryker Inc., Michigan, USA)

result, due to the navigation and assistance of the robotic arm in this system, the outcome improved considerably and this system is known as a valuable platform for surgeons[27].

1.1.4 Robotic systems for cardiac ablation surgery

As described earlier, ablation surgery has been known as the most promising and acceptable method for treating AF. This surgery usually performs under x-ray exposure using some devices such as catheters, guide wires and sheaths[28]. The skill of the surgeon in maneuvering the catheter to reach the spots of interest and also haptic feedback are important factors in this surgery[29]. To increase safety, and operation improvement in some cases and also reduce the radiation risks, the master-slave robotic systems have been developed[30, 31, 32]. Biase *et al.*[33] conducted a clinical study among 390 patients to compare manual ablation therapy using conventional catheters with robotic-based catheterization systems. The final findings indicate that the success rate in the robotic navigation system is slightly higher than manual ablation and also fluoroscopy time was considerably lower in robotic-based operation. Due to the promising results of mentioned platforms, in recent decades, ablation control systems have been approved by FDA as a safe and effective

Table 1.1: Commercially available robotic-assisted ablation surgery systems

System	Company	FDA approval*	Specifications
Sensei	Hansen Medical, Inc.(USA)	2008	A custom-designed steerable catheter is implemented in an electromechanical system and the surgeon actuates the catheter with a 3 dimensional joystick
CorPath	Corindus Inc.(USA)	2012	A manipulation system actuates a standard catheter into the body and it can be controlled remotely by dedicated joysticks of its console
Amigo	Catheter Precision Inc. (USA)	2012	3 degrees of freedom manipulator that uses a standard catheter controlled by a remote handle similar to a conventional catheter's handle
Niobe	Stereotaxis Inc. (USA)	2002	A magnetically controlled system consisting of a specially designed catheter that is steered remotely by the magnetic field around the patient

* The approval date in FDA database

method for the treatment of AF.

On the master side of the robotic platforms, the surgeon operates the console by hand joysticks or foot pedals to control the mechanical mechanism on the slave side. Moreover, the console's monitors provide different views of the patient's body with some essential data, such as the parameters of the RF generator. On the slave side, regarding navigation technology, robotics-based AF surgery is classified into two kinds of platforms. The first one uses magnetic field vectors to control the position of the catheter inside the patient's body. In this system, external magnets actuate the custom-designed catheter. On the other hand, the second platform utilizes electromechanical mechanisms to operate the standard available catheters. In this system, a mechanism steers a catheter similar to the movements of the surgeon's hand. Table.1.1 compares some available commercial systems in this area:

The *Sensei* robotic system is a master-slave platform consisting of a mechanism mounted on the operating room's table to control a catheter and also a 3-DOF hand-operated joystick on the console side. The electromechanical unit steers a dedicated guide sheath (a flexible hollow tube) into the

cardiac system to reach the spot of interest and then it inserts a standard catheter for the operation such as ablation[34]. This system provides catheter stability during the procedure but because of the rigidity of the guide sheath, the mechanical complication is a noticeable risk[35].

The *CorPath* as a robotic system for cardiac intervention allows the physician to sit in a shielded area to actuate a catheter inside the patient's body by joysticks. In addition, the catheter or guide wire(a solid flexible wire for the guidance of insertion) can only be maneuvered with a customized mechanism, which is not compatible with all types of cardiac catheters.

The *Amigo* is a remotely controlled system including a mechanical assembly mounted on the patient's table and also a handle that mimics the standard catheter's handle. The user in a radiation-safe environment can hold the remote controller similar to the handle of conventional catheters and perform the surgery. This handle system can provide force feedback information of the catheter's tip contact force if it is equipped with sensor-embedded catheters[36].

The *Niobe* system is a magnetically guided setup that two external magnets on two sides of the patient navigate the custom-designed catheter. Navigation of the catheter with embedded magnets can be achieved by moving and rotating the large external magnets to change the magnetic field vectors. The *Niobe* catheter is soft and reduces the risk of perforation compared with standard catheters, but it takes longer to ablate[37].

In this section, well-known robotic platforms for cardiac ablation have been briefly reviewed but important parameters corresponding to the perfection of ablation spots have not been considered. In the following section, considerable parameters for the success of ablation surgery will be mentioned.

1.1.5 Ablation lesion's formation and importance of contact force

During the radio frequency (RF) ablation, the generated thermal energy is delivered to the heart tissue, resulting in destroying(ablation) the area under the catheter's tip(electrode)[38]. In this procedure, the surgeon activates the RF generator device for a defined period when it is confirmed that the catheter's tip has the proper contact with the tissue. The success of ablation is associated with the proper lesion size and the main goal of ablation is to create an optimal volume of lesion[39]. There are different methods to increase the lesion size during the ablation such as enlarging the electrode's diameter and increasing the temperature of tip[39]. The larger diameter needs a higher

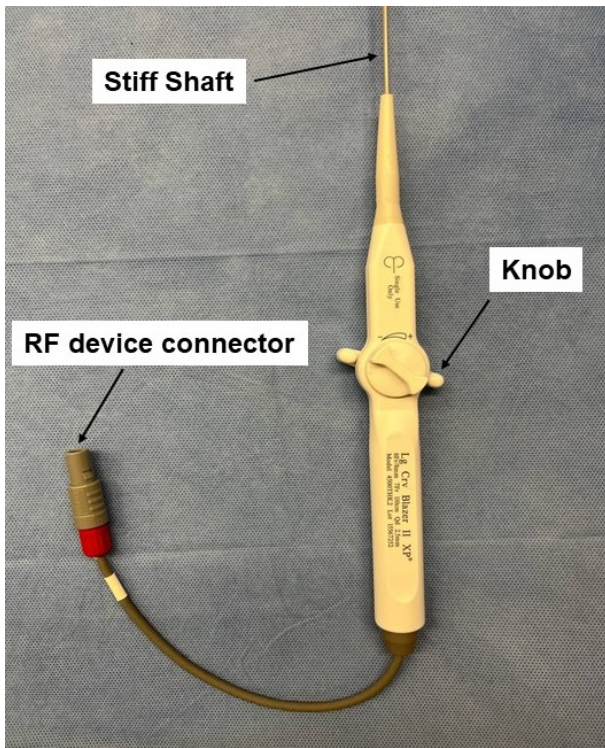
power source to increase the lesion size, although biological features such as tissue thickness, tissue structure, and blood flow can affect on tip's scar on tissue.[40] More clearly, if the larger electrode is used, the higher temperature should be set, and also for the smaller electrode, the physician should increase the temperature to finally ablate more volume under the tip. Although increasing the temperature can ablate more tissue volume, this method has a limitation known as "steam pop". In this condition, if the tip's electrode reaches 100°C, intramyocardial steam will be formed causing cardiac perforation [41].

Despite the fact that the above-mentioned parameters affect the formation of the lesion, another significant factor which is catheter-tissue contact force (CF) is a key to control the creation of ablated spots[42]. Clinical studies show that CF is a determinative feature of lesion creation and also its proper control engenders the sustainability and success of the treatment[43, 44, 45]. The reason behind the importance of adequate CF is that the electrical current passes more efficiently into the tissue to create the ablation scar and also the electrode sliding will be reduced, leading to improved tip localization [46].

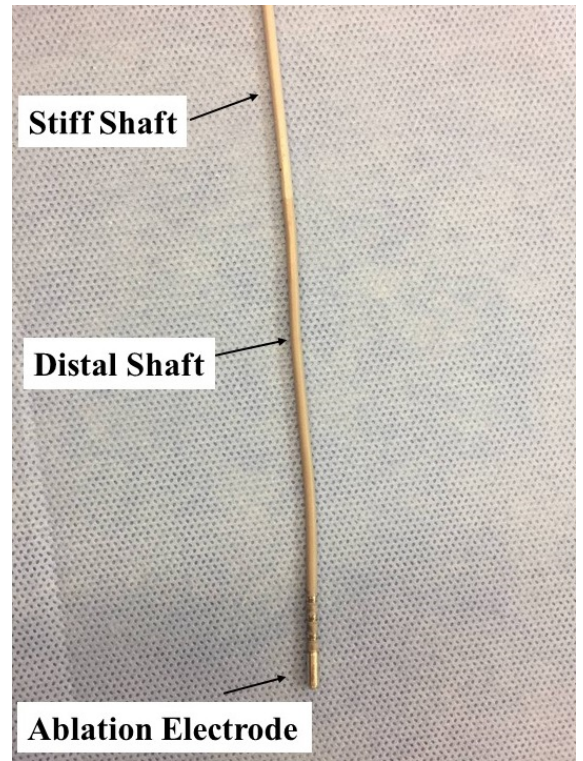
As described in the previous sections, during the ablation procedure, typically the physician steers a sheath (a hollow flexible tube) by insertion, handle rotation, and knob actuation manually or remotely to reach the target spot. Afterward, the ablation catheter will be inserted to apply the force to the target consequently. Figure 1.7(a) illustrates the handle of a bi-directional ablation catheter (Boston Scientific Blazer II XP) in which the knob is for the actuation of the catheter's tip and distal shaft. The distal shaft of this catheter, shown in Figure.1.7(b), is actuatable in 2 directions that helps the surgeon to steer the catheter correctly. And also, Figure.1.7(c) depicts a hollow sheath(Boston Scientific DIREX steerable sheath) that should be inserted before the ablation catheter which has the same mechanism and structure.

1.1.6 Problem definition based on the clinical need

According to mentioned clinical reviews and studies, the CF plays an important role in the ablation procedure. It is a key parameter in the formation of the lesion and its proper control helps the physician to reach more stable and efficient results. As reported in experimental studies, the CF between 0.1*N* and 0.3*N* is known as the safe and effective range for ablation [39]. Excessive force



(a)



(b)



(c)

Figure 1.7: Ablation Catheter and steerable sheath- (a): Standard ablation catheter's handle(Boston Scientific Blazer II XP) - (b): Different sections of the shaft of ablation catheter - (C): Steerable ablation sheath(Boston Scientific, USA)

can cause failures such as tissue perforation and also inadequate contact will reduce the efficacy of the procedure significantly [33].

Consequently, the need for a real-time sensing system is tangible to provide accurate force measurement for the surgeon. Furthermore, in robotic systems, a force control platform can be implemented to assist the surgeons in applying the force to the spot of interest. This force controller system sends commands to a robotic mechanism to insert the catheter to reach the desired force. This controller benefits from the method of force sensing or estimation, meaning that firstly a method should provide the force and then feed it to the controller's logic to actuate the robotic mechanism for the catheter insertion.

In the following section, different technologies and methods for force sensing and estimation have been classified. Each modality has been reviewed and finally, the method of the choice for this thesis will be explained. In the end, the utilization of the introduced force sensing method will be described in a controller.

1.2 Literature Review

To monitor the applied force in the catheter ablation procedure, different methods have been introduced. In general, these methods fall into two categories: 1- Sensor-based ,and 2- Sensor-free[47, 48]. The first approach involves embedding a tiny sensor at the tip of the catheter that detects CF. On the other hand, in the sensor-free technique, based on the analysis of the shape of the catheter's distal shaft under applied forces, the force is estimated.

Each of aforesaid methods has its benefits and also limitations. Sensors provide accurate measurement but the use of sensors in the unstructured environment of the heart chamber is challenging[49]. Generally, catheters are dispensable and the use of costly sensor-embedded catheters is not affordable. Accordingly, sensor-less techniques recently have caught attention in the literature[47]. In this manner, the deflection of the distal shaft of the catheter is analyzed. Because of the flexibility of the distal shaft, it bends under applied forces, so it is an insight to model the catheter's behavior to estimate the force. The challenge of this method is the mathematical complexities in some cases but this method is considerable and beneficial because it just relies on standard available catheters.

In the following sections, some available solutions for the force sensing of ablation catheters are reviewed and compared together.

1.2.1 Sensor technologies

In an effort to improve RF therapy, microsystem technologies have been developed over the past few years[10]. The main goal of this technology in AF treatment is to use tiny sensors for providing haptic feedback to the surgeon. As shown in clinical studies, using catheters with a sensor is associated with more safety and a higher success rate[50]. Furthermore, catheters with sensing capabilities accelerate the surgery, resulting in less X-ray exposure[51].

In 2014, *St Jude Medical* company developed the *TactiCath*TM catheter that the fiber-optic technology is implemented to make a contact sensing capability. The sensing system (*Tactisys*TM quartz equipment by *Abbott Medical* company) analyzes the reflected light from the optical fibers of the catheter(Figure.1.8(a)) to determine the applied force. By deformation of the optical package upon contact with tissue, the wavelength of the light in fibers is changed and it correlates with the angle and magnitude of CF [52]. Therefore, the surgeon not only monitors the orientation of CF but also detects the strength of the applied force in a real-time manner.

The *Thermocool Smarttouch*TM catheter developed by *Biosense Webster* company is another commercially available catheter with CF sensing capability. As illustrated in Figure.1.8(b), 3 location sensors measure the distance with a magnetic transmitter coil. The lateral and axial forces of the tip are calculated based on the deflection of the spring in the sensor[53]. The CF measurements are displayed on *Cartounivu*®mapping system (by *Biosense Webster* company)[54].

The mentioned catheters do not show the quality of the ablation and characteristic of the tissue. To this end, *Directsense*TM technology has been introduced by *Boston Scientific* company that is based on the electric field around the catheter's tip to display the electrophysiologic information for the physician. The concept of this technology is inspired by the electric fish that generates an electrical field around its body to detect and sense obstacles. In the *Directsense*, As shown in Figure.1.8(c), a similar electric field is generated around the catheter's electrodes and the mapping system calculates the local impedance that is the indicator of catheter-tissue contact and the quality

of the ablation procedure[55]. As mentioned in the reviewed clinical studies, haptic feedback significantly improves the AF treatment because it allows the surgeons to have a sense of touch. In this regard, *Directsense* system can be a valuable supplement for the CF sensing catheters that makes the AF treatment more successful and accurate.

Catheters with embedded sensors provide valuable information that positively affects the outcome of AF therapy but they have some limitations[49]. Firstly, because of the technology of sensor-based catheters, they are costly and the fact that they are disposable, makes this issue more remarkable. Also, the calibration and data acquisition in an unstructured environment are challenges of this technology. To this end, sensor-free methods caught the attention of the literature and in recent years many developments and innovations are introduced in CF estimation of standard catheters. The following section will cover these methods.

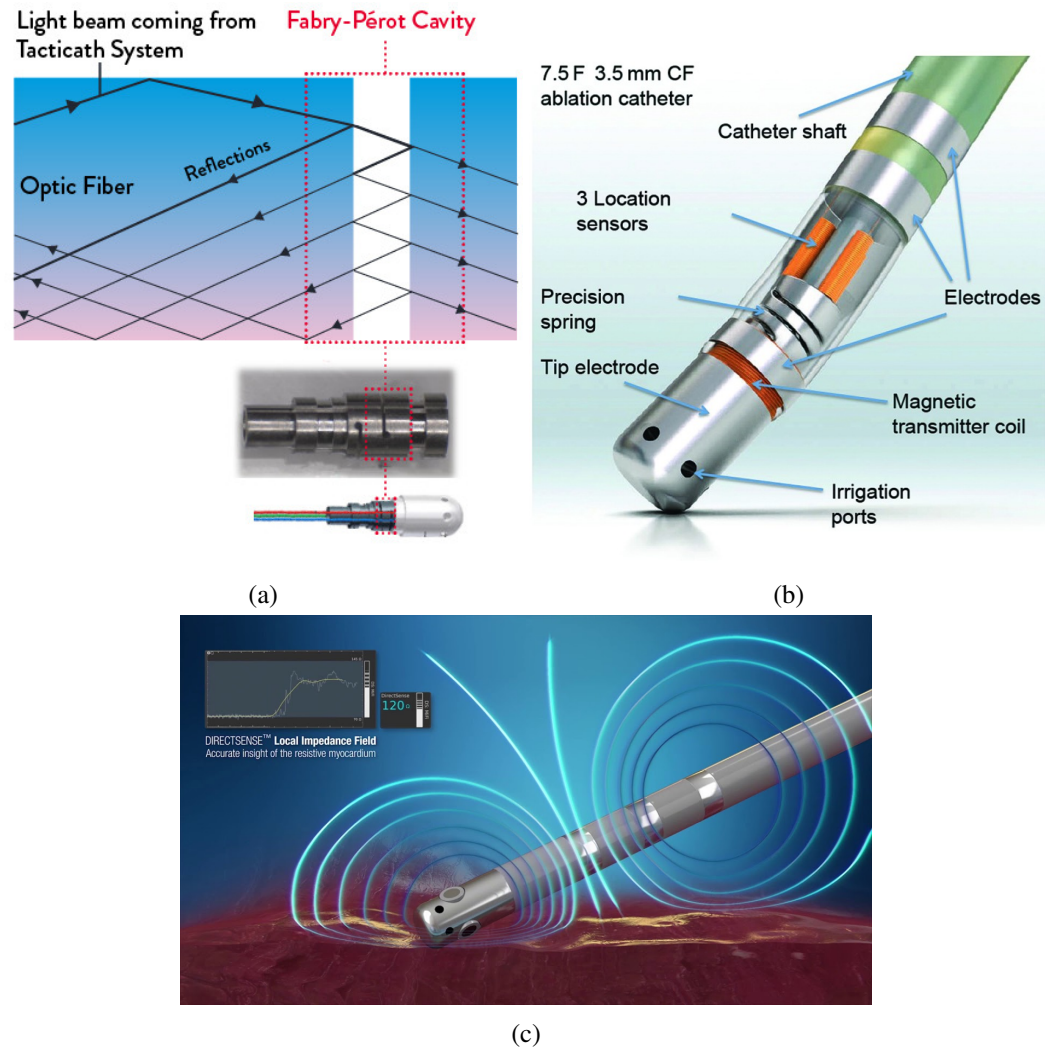


Figure 1.8: Commercially available sensing technologies of ablation catheters- (a):TactiCath™ contact force ablation catheter(Abbott Laboratories, Abbott Park, Illinois, USA) - (b):Thermocool®catheter(Biosense Webster Inc., California, USA) - (c):Directsense™ technology (Boston Scientific Corporation, Marlborough, Massachusetts, USA)

1.2.2 Mechanical model methods

As elaborated in the previous sections, CF sensing plays a positive role in AF treatment. The model-based approach in recent years has been investigated and evaluated to estimate the CF of standard catheters. This method is based on the deflection of the shape of conventional available catheters and the implementation of physical modeling theories. This solution requires some elements including machine vision algorithms, model algorithms, and optimizers. The extracted model should be accurate enough, robust, and also fast to provide CF in a real-time manner [56]. In this method, an image processing algorithm should be employed to extract the catheter from the input image. The input image can be the X-ray type or an image of a camera from an experimental setup. After calibration of the imaging system(camera), the segmentation algorithm should be deployed to detect the catheter's distal shaft from the input image and provide some features for the modeling phase. The extracted features could be geometrical information such as pixel's location or Cartesian coordinates values. For instance, the pixel's location of the catheter's tip is extracted and converted into Cartesian coordinates or the slope of different points at the body of the catheter can be calculated. Afterward, the data from the image processing phase should be passed to the input of the developed model to estimate the CF. Usually, parameter identification and optimization algorithms are necessary to make the model precise and realistic. To evaluate the developed model, an experimental setup is required to compare the results of the model with the actual values. The experimental setup generally is an electromechanical system to apply the force to a catheter and in order to record the data, a DAQ system is required. Various techniques have been introduced to model a catheter for CF estimation such as continuum mechanics, multi-body dynamics, differential geometry, and particle-based models [19]. Following is a summary of the mentioned models.

Robotic arms are a discrete system of rigid links that are controlled by actuators at each link's connection or joint. These actuators are indicators of the degree of freedom for the system and in an attempt to design a robotic system to produce a curve-like shape, many actuators should be deployed. Due to the geometrical characteristic of this snake shape, many actuators should be implemented. Using these actuators increase the size of system that is not ideal for cardiac intervention. So, the alternative system is continuum robots that they bend along their length and an example of

this method is the steerable catheters. The *Continuum mechanics model* is an analytical approach whose main assumption is to describe a manipulator as a continuous mass. In this modeling modality, the tendon-driven catheters are considered as a continuum manipulator that is modeled as a cantilever beam in which the tendons control the deflection [57]. In early studies in 2005 and 2008, Bailly *et al.*[58] and Camarillo *et al.*[59] both implemented continuum modeling to predict the cardiac catheter's shape but the main limitation is that they are computationally expensive and cannot be used in a real-time manner. In other studies by Khoshnam *et al.*[60], [61] and [62] in an attempt to design a model for force-position control, the catheter modeled based on a large deflection beam theory. Although this model is capable of estimating the shape independent of the internal structure of the catheter, the solution is just developed for 2-dimensional mapping of applied CF at the tip.

Multibody dynamics is another computationally efficient modeling method to analyze the deformation of catheters. In this technique, the system is assumed to have various rigid bodies in which they are attached by joints or springs [63]. In this method, the identification of constant parameters is indispensable to provide the acceptable result [64]. In one early study Alderliesten *et al.* [65] used the multibody dynamics method to simulate vascular intervention for training the operator. To show the feasibility of the simulation, it was tested on an experimental phantom and patient data. However, this study is performed in 2-dimensional space and also it is assumed that the speed of maneuvering is slow.

Differential geometric as a mathematical method is described as a technique based on the position of some points to estimate the system. Polynomial interpolation is an example of this method [19]. The Cosserat rod is one of the well-known theories in this modeling approach that is used for modeling of catheters. Tang *et al.*[66] used the Cosserat rod model to evaluate a hybrid solution for cardiac guide wires in such a way that the body of the catheter was modeled by Cosserat rod and the distal tip by a beam theory. The results showed promising accuracy in a real-time simulation but the accuracy is dependent on the optimization algorithm. In the other recent study, to estimate the CF of ablation catheters, an inverse solution of the Cosserat rod model was implemented and the model accurately estimated the CF [67]. However, in the mentioned study, the out-of-plane deflection is a concern that can directly effect on the accuracy of the estimation.

Particle-Based dynamics modeling known as the mass-spring model, usually is used to describe

the deformation of the tissue in the vascular intervention. Lenoir *et al.* [68] introduced a solution that the vascular tissue is assumed as a rigid body and catheter modeled to detect the collision in intervention. In this study, Newton's law has been used to have motion equations. However, the particle-based modeling does not provide physically admissible results [61].

The mentioned modeling methods provide acceptable accuracy in some cases and also it is noticeable that the sensitivity to the noise in comparison to the sensor-based approach is low. Furthermore, the model-based method is affordable because the conventional standard catheter is used and it does not need to redesign the catheter. On the other hand, the main limitation of this modality is the uncertainty of the solution due to model parameters [69]. Usually different parameter identification and optimization algorithms should be deployed to have an optimal model with acceptable accuracy.

1.2.3 Learning-based estimation

To overcome the limitations of the model-based estimation, the machine learning approach has been implemented in recent years for cardiac intervention. Mechanical models are complex due to many parameters that should be identified. In order to have an accurate model, optimal parameter identification is highly important. In addition, the speed of CF estimation is an important feature and in some types of models the speed of calculation is not fast enough to provide the force quickly. To this end, the learning-based method does not need mechanical calculations and just deals with input data that can be an image or some geometrical features. The final estimator can be capable of providing the CF quickly and accurately.

Support vector machine(SVM) and artificial neural network(ANN) are well-known machine learning models that have been utilized for regression or classification problems. In regression problems, the model tries to find the best fit of training data for the optimal solution. On the other hand, in the classification approach, the model determines the best available class of possibilities for the system. In the supervised learning method, the model should be trained by a set of available data. Usually, to build a dataset for the training, an experimental setup or a simulation is required. After gathering data, the data cleaning process is essential to overcome redundant and out-of-range data points. To improve the correctness and reduce the redundancy of data in the same scaling

format, the feature scaling process is required. In this statistic adjustment, the data should be scaled into a defined range. For example, in *Mean normalization* technique, the mean of whole data is calculated and the new dataset based on the equation.1 is calculated. In the mentioned equation, x' is the scaled data from the original value of x . Equation.2 shows *min-max normalization* method as the other method of feature scaling that scales the data in the range of [0,1].

$$x' = \frac{x - average(x)}{max(x) - min(x)} \quad (1)$$

$$x' = \frac{x - min(x)}{max(x) - min(x)} \quad (2)$$

After preparing the data, the appropriate machine learning model should be selected for the training. Usually, to evaluate the final trained model, the whole data should be split into two or three sets including training, evaluation, and test sets. The training set is the most portion of the dataset and also test set, known as unseen data, is for the evaluation of the trained model. In some cases, to examine the accuracy of the model during the training, the evaluation set is utilized. [Figura.1.9](#) depicts the overall process of the machine learning procedure.

As illustrated in [Figure.1.9](#), the final trained model has been fed with features that come from the dataset to estimate parameter(s). For instance, in the case of CF, the input can be some geometrical features of the X-ray image of the catheter to estimate the CF as the output. To build a dataset of features, a feature extraction algorithm is required. In the case of CF estimation, the feature extraction is some information of the X-ray medical image or standard colored image from the camera of the experimental setup. To this end, DAQ system is required to record the data and make the dataset ready for the next step of the analysis. To this end, a sensor records the force data and a camera captures images of a catheter under different applied forces. An image processing algorithm extracts some unique features from each image and the corresponding force data of the sensor is stored in the dataset. This is one form of data gathering process that finally the trained model is capable of estimating the CF based on the features of the image. In other words, a camera capture a video from the ablation surgery and the estimator reports the CF for the surgeon based on every frame of the video. Depending on the feature extraction algorithm calculations and model structure,

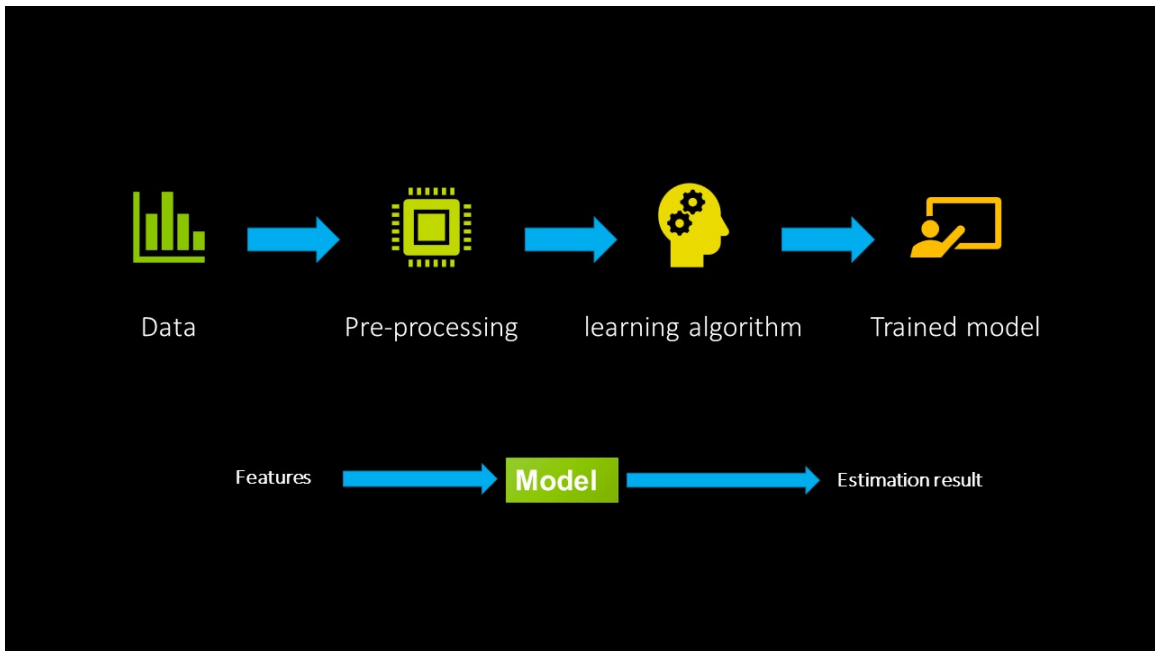


Figure 1.9: Machine learning procedure

the result of CF will be displayed simultaneously.

Following is a review of studies in which machine learning methodology has been deployed and finally, the overall contribution of the thesis will be introduced.

In mechanical analysis, machine learning models can be a complementary component to overcome nonlinearities that sometimes are neglected. Runge *et al.* [70] implemented an ANN to train a model for the forward kinematic of a soft robot. This work is the combination of finite element simulation, mechanical kinematic analysis, and ANN. The soft robot was simulated to extract kinematic parameters and the corresponding loads. Finally, an ANN was deployed to map parameters for the kinematics of the robot. However, the accuracy of the final model highly depends on the correctness of finite element simulation that material properties and manufacturing aspects play an important role. In another study, Jolaei *et al.* [71] proposed a control framework for positioning the tip of a tendon-driven catheter. In this method, a classifier and a regressor were utilized as alternatives to the inverse kinematic solution in an attempt to deal with mechanical nonlinearities. In this regard, based on the desired position, an SVM classifier determines the proper tendon to be actuated and then an ANN regressor estimates the required tendon's length but this system is not capable of

real-time actuation.

In robotic catheter intervention systems, the surgeon usually uses the joysticks of the console to steer the catheter by rotation and insertion movements. To transfer the rotational movements in haptic-enabled systems from the master side(joystick), typically an inertial measurement unit(IMU) is deployed to monitor the orientation based on changes in roll, pitch, and yaw angles. To report the spatial orientation of an object equipped with IMU sensors, the integration of angular velocities is required. Due to noises of measurement in the IMU sensor and accumulative effect of the integration over the time, finally, the calculated orientation will not be accurate enough. To tackle this issue, Hooshiar *et al.*[72] introduced a learning-based approach to estimate the spatial orientation needless of integration. To this end, a three-layer feedforward ANN was trained based on roll and pitch angles to determine the corresponding yaw angle for estimation of the orientation. For this study, a wearable device equipped with two IMU sensors was designed to be used in catheter steering systems but the proposed system requires more developments regarding the fault detection of the sensor's data.

To estimate the CF of ablation catheters based on learning methodology, a dataset of proper features should be gathered. The manipulation of a dataset is commonly accomplished through experimental setups or computer simulations. Sayadi *et al.*[73] modeled an ablation catheter in a finite element simulation software to record CF in different conditions and eventually a learning-from-simulation method was introduced. To arrange a dataset, 4 control points based on Bezier spline shape interpolation were extracted for every deformation of the catheter under applied forces. The extracted features(control points) were fed into commonly used machine learning models(ANN and SVM) to estimate the CF. Although this study reported an accurate estimation of the CF, the simulation parameters identification and the validation of the model are still challenging. On the other hand, by using an experimental setup, a real-world dataset can be arranged. To solve these issues, an experimental setup was used by Nourani *et al.*[74] to propose an image-based method for feature extraction based on polynomial interpolation of the catheter's curvature. In this study, an experimental setup was used to apply a range of forces on the tip of a standard catheter and the corresponding image of the distal shaft was captured. The distal shaft was considered as a mathematical function similar to a polynomial that each deflection has unique coefficients. An image

processing algorithm was deployed to segment the catheter from the background of the captured image and then the best mathematical curve was fit to the distal shaft's shape. To extract the features for the learning phase, polynomial coefficients of each curve which is a catheter's distal shaft deformation under an applied force, were calculated. To build a CF estimator, coefficients were utilized to train an SVM. Overall, this solution is not computationally efficient as it should compile an image processing algorithm alongside a mathematical calculation for curve fitting. However, the proposed method introduced some insights into using the image data(pixels) for the learning step. In another study, Feng *et al.*[75] designed a catheter based on the continuum robot's principle in an attempt to estimate the CF by a learning model. In this research, a tendon-driven catheter was designed in which the tendons were actuated by servo motors and the tension was measured by the load cells. Displacement and pulling force of the tendons were recorded as the input of a neural network model to estimate the CF in two directions. This method estimates the force regardless of the mechanical properties of the catheter. Nevertheless, it requires some features that should be measured by sensors, meaning that this estimator is just functional for a custom-made catheter.

All in all, the learning-based estimation recently has caught the attention in the literature because of the acceptable accuracy, less computational time, and less modeling complexity. The evaluated model finally can be implemented in a control loop for a robotic system to apply the force accurately and safely on a tissue. In this regard, the motivation and objectives of the thesis are introduced in the following section.

1.3 Objectives

The main motivation of the present thesis is to develop a robotic system to maintain the catheter-tissue contact force at a desired value based on a vision-enabled and learning-powered estimator for the problem that was mentioned in Section 1.1.6. To this end, the objectives of this research are:

- To develop a sensor-free and vision-based method for estimating the CF of commercially available ablation catheters accurately in a real-time manner. This technique should be just based on the images of the distal shaft of the catheter for a machine learning model.
- To develop a fast and precise controller by a machine learning-based force feedback estimator

to apply the desired force. A catheter manipulator should be designed to actuate the catheter for the control signals.

- To design an adaptive vision system capable of providing a fixed view of the target area of the ablation. This system functions simultaneously with the actuation of the designed catheter manipulator.

1.4 Publications

This section presents the publications of the author during the master of applied science research:

- **Hamidreza Khodashenas**, Pedram Fekri, Mehrdad Zadeh, and Javad Dargahi. "A vision-based method for estimating contact forces in intracardiac catheters." In 2021 IEEE International Conference on Autonomous Systems (ICAS), pp. 1-7. IEEE, 2021.
- Fekri, Pedram, **Hamidreza Khodashenas**, Kevin Lachapelle, Renzo Cecere, Mehrdad Zadeh, and Javad Dargahi. "Y-Net: A Deep Convolutional Architecture for 3D Estimation of Contact Forces in Intracardiac Catheters." IEEE Robotics and Automation Letters 7, no. 2 (2022): 3592-3599.
- **Hamidreza Khodashenas** and Javad Dargahi, "Force control on intracardiac catheters by using neural force estimation", **Submission process**

1.5 Thesis layout and contributions

This thesis is organized in manuscript-based style according to the *Thesis Preparation and Thesis Examination Regulations for Manuscript-based Thesis* of the School of Graduate Studies of Concordia University including following chapters:

Chapter 2: describes the data collection process and experimental setups design for the present thesis. As mentioned in the first objective of the thesis, a machine learning model should be deployed to estimate the CF from the image of the distal shaft. To this end, an experimental setup

is required to collect images and corresponding forces to make a mapping between the images of the distal shaft and the applied forces. An experimental setup was designed and implemented consisting of camera, actuators, and force sensor to compile the datasets for the training of machine learning models. The concept of the design of data collection setups was inspired by a research thesis at robotic surgery laboratory of Concordia University, Nourani *et al.*[74]. After organizing the datasets, a 3 DoF catheter manipulator was designed and deployed for the vision-based control of CF. This mechanical mechanism is based on the design concept of commercially available surgical robotic systems mentioned in section 1.1.4 and was used in **Chapter 4**. The compiled datasets by the author of the present thesis were used in all mentioned contributions in the previous section (1.4). It is notable that just the uni-planar setup was used in the **Chapter 3** and **Chapter 4** for training of models.

Chapter 3 presents a sensor-free and vision-based method for estimating CF in ablation catheters. In this method, an image processing algorithm was developed to extract features from the image of the distal shaft of the catheter to be used as the inputs of the machine learning models. ANN and SVR models were implemented in this study to compare the accuracy and feasibility of the estimation. The input of the models is the features extracted from a pre-processing phase and the output is the estimated forces. The proposed method showed benefits over the previous studies in the literature and due to the fast estimation of the models, they can be used as a feedback element in a control loop. This chapter is based on a published manuscript in the *2021 IEEE International Conference on Autonomous Systems (ICAS) hosted at Concordia University*:

- Hamidreza Khodashenas, Pedram Fekri, Mehrdad Zadeh, and Javad Dargahi. "A vision-based method for estimating contact forces in intracardiac catheters." In *2021 IEEE International Conference on Autonomous Systems (ICAS)*, pp. 1-7. IEEE, 2021.

The second author of this paper contributed in model preparation and evaluation. The Third and fourth authors are academic supervisors.

Chapter 4 presents a control system to maintain the CF at the desired value by using an adaptive mono-planar imaging system and a learning-based feedback element. This controller showed the possibility of using learning-enabled estimators as the force feedback element in the control loop.

An optimized trained ANN model was used for this controller and it was evaluated for both static and dynamic desired forces. To provide a fixed view of the camera for the model, a robotic arm was deployed to hold the camera in a fixed location from the distal shaft. The robotic arm was capable of moving according to the actuation of the catheter's manipulator. This chapter is based on a manuscript that is in the submission process:

- Hamidreza Khodashenas and Javad Dargahi, "Force control on intracardiac catheters by using neural force estimation",

The second author is the academic supervisor. Note that this paper is in the submission process and the final manuscript will be available after modifications based on the IEEE conference paper style.

Chapter 5 concludes the thesis and provides a summary of results. In the end, potential future research in continuation of this master of applied science research are mentioned.

Chapter 2

Data Collection and Experimental Setup Design

2.1 Introduction

In an attempt to analyze the CF behavior during heart ablation surgery, this procedure should be imitated through an experimental setup or simulation software. This chapter is focused on the use of experimental setups for the CF study. Firstly, different types of setups in the literature were reviewed briefly and then the designed systems for this thesis will be introduced in detail. A uni-planar data acquisition setup was designed and implemented in this thesis to compile a dataset of images and corresponding forces for the training of machine learning models. This system is a vision-based setup consisting of a camera, an ablation catheter, a force sensor, and an actuator. In the uni-planar system, just one camera was implemented to capture the image from the catheter's distal shaft. The camera was utilized to simulate the X-ray machine during the ablation surgery that tracks the movement of the catheter. The actuator in the setup was used to apply the force or to make periodic movements similar to the heart beating. This setup has been used for data acquisition for the training of machine learning models and finally, a force control system is designed to evaluate the performance of the models as the force feedback element. At the end of this chapter, based on available commercial cardiac intervention systems, a robot will be introduced that is designed to implement the machine learning models in a control loop for the CF control.

Data for a machine learning model should be gathered accurately and correctly. To this end, the force sensor should be accurate enough to measure small force variations, and the catheter should be actuated precisely. In this regard, some experimental setups have been designed and implemented for the evaluation of proposed models in different types of modeling approaches. In general, researchers fall into two groups in terms of designing the setup. On one hand, they design a catheter from scratch, meaning that they prototype a flexible tendon-driven shaft similar to the standard catheters. On the other hand, the actual standard catheter can be used for the experimental evaluation of the study.

In this chapter, firstly some available academic setups are reviewed and then experimental setups of the present thesis will be presented and the collected data will be illustrated. Some details about data collection algorithms and different components of the setups will be explained thoroughly.

2.2 Review of available setups

Experiments have been conducted using either actual standard catheters or customized catheters to evaluate the catheter's CF models. In the first category of setups, Jolaei.*et al.* [71] and Hooshiar.*et al.* [67] fabricated a tendon-driven catheter named as *MiFlex* based on the geometrical features of a standard 18-Fr (Each Fr= 1/3 mm diameter) catheter. This continuum robot was actuated by 4 tendons that are attached to stepper motors. In addition, the rotary potentiometers were deployed to measure the tendon's length. Two USB cameras capture images of the catheter from the top and side view to feed them to a user interface (UI) software in the computer. This flexible catheter was fabricated with a silicon rubber material and a coil spring was used to reform the catheter's shape after actuation. This design principle has been used in other studies by different researchers to test the analytical approaches or control frameworks. In the customized design approach, Back.*et al.*[76] and [77] used a helix flexible structure as a continuum robot to evaluate a three-dimensional model of force. In these experiments, the USB camera was used to capture images of the catheter under applied forces and also a force sensor was deployed for parameter estimation and evaluation of the final equations.

As another option, the actual medical catheter can be used in the experimental setup. Khoshnam.*et al.* [62] used a 7-Fr standard catheter to design a control system for CF but in this research, a custom-designed optical sensor was attached to the distal shaft of the catheter to monitor the tip angles. The tip angle based on the analog voltages of the sensor was estimated and then the data from the sensor provides the necessary parameters of the control loop. The researcher also used the standard catheter without the mentioned sensor to evaluate the mechanical modeling approaches[60, 61]. In addition to these studies, Hasanzadeh.*et al.* [69] and Kouh.*et al.* [78] used a standard catheter for the experimental analysis of CF. Instead of using the camera to track the catheter, the researchers used a magnetic field generator device to track the catheter's location using a magnetic sensor attached to the tip. Using a medical catheter without any attached sensor is a method of the choice for recent studies. Nourani *et al.*[74] used a standard catheter to build a dataset for a proposed model. The camera stores images of the catheter under different applied forces and a multi-axis force sensor measures the corresponding forces of each image. A linear actuator was installed to apply forces to the tip. In the end, a machine learning model estimates the CF based on the provided data. In a similar modeling principle, Sayadi.*et al.*[73] developed a simulation of an ablation catheter and for assessment of the simulation and a proposed method, a standard catheter was used to perform different CFs. In One recent study, a bi-planar imaging setup for data collection and estimation of the force in 3 directions was implemented [79]. This experimental setup is based on the uni-planar setup of the present thesis to capture images and corresponding forces. In this experimental setup, two cameras were installed perpendicularly to capture a pair of images for the applied force. One camera was installed in a location to capture the bending section of the distal shaft of the catheter and the other one records the out-of-plane bending. The force sensor in the setup collects the 3 components(x, y, z) of the applied force. The compiled dataset consisting of the pair of images and the corresponding force components was used to train a convolutional neural network known as "y-net" to estimate the CF by the researcher of the study.

To address the defined problem in CF assessment during the ablation procedure, an experimental setup is required. The objective of the present thesis is to develop an image processing algorithm to segment the catheter from the image and extract the features for machine learning models. So, with this objective in mind, a setup consisting of a catheter, a camera, an actuator, and a multi-axis force

sensor should be implemented. It is noticeable that the only input of the system should be an image from the distal shaft of the catheter, so there is no need for tracking markers or sensors. Ultimately, a robotic insertion mechanism should be deployed to perform CF control in different modes.

In the following sections, firstly the design principle of a uni-planar imaging setup will be explained in detail. This setup is uni-planar as just one camera was used to capture images. The proposed models of the thesis will be based on the collected data of this setup and will be explained in *Chapter.3* completely. The final section will be the introduction of a robotic system for catheter insertion and CF control that is based on commercially available catheter manipulators.

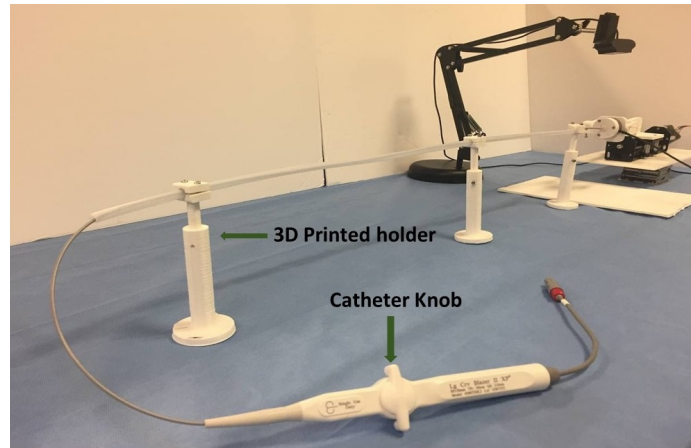
2.3 Uni-planar imaging setup

In an attempt to collect samples for training a machine learning model, an experimental setup was designed. The present setup was inspired by the system that was utilized in a study of CF by Nourani.*et al.*[74]. The setup is called uni-planar as just one camera is implemented to capture the images of the distal shaft from one side of view. The camera was used to imitate the X-ray fluoroscopy machine in the ablation surgery. As shown in *Figure.2.1*, a c-arm mechanism provides X-ray images for the surgeon during the ablation surgery. *Figure.2.2* shows the overall view of the setup consisting of sensing and actuating components. In this assembly design, the USB camera(Logitech C920) plays the role of a X-ray machine (fluoroscopy) to track the curvature of the distal shaft under applied forces to the tip. A medical ablation catheter (Boston Scientific Blazer II XP) was inserted into a plastic hollow sheath. This tube mimics the steerable sheath that during the ablation surgery, the physician inserts into the cardiac system to reach inside the heart. The 3D-printed adjustable holders fix the sheath to a rigid plate or table. The catheter's knob was adjusted to the neutral position in which the tendons are not under agonist-antagonist tension. The distal shaft is in contact with a multi-axis force sensor(ATI Mini40) that measurements are transferred to the computer by a data acquisition device (National Instruments, USB-6211). The camera is calibrated and fixed to just record the view of the distal shaft(flexible part). To apply force to the catheter's tip, a linear actuator mechanism was assembled using a stepper motor(17HS4401-S 40mm Nema) powered by a micro-step driver(HANPOSE TB660).

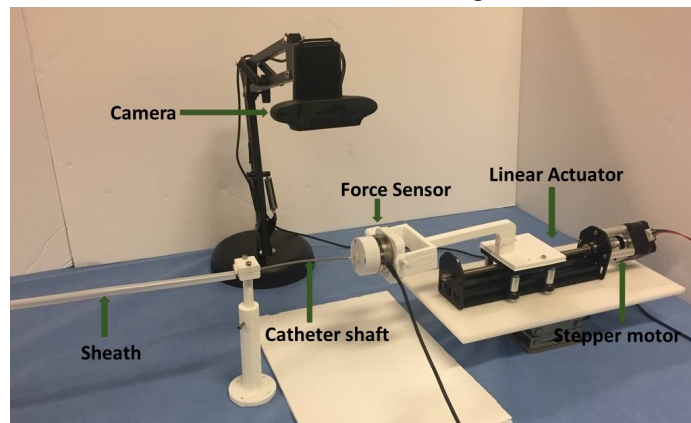


Figure 2.1: Fluoroscopy system Allura Xper FD10 - Philips, Netherlands

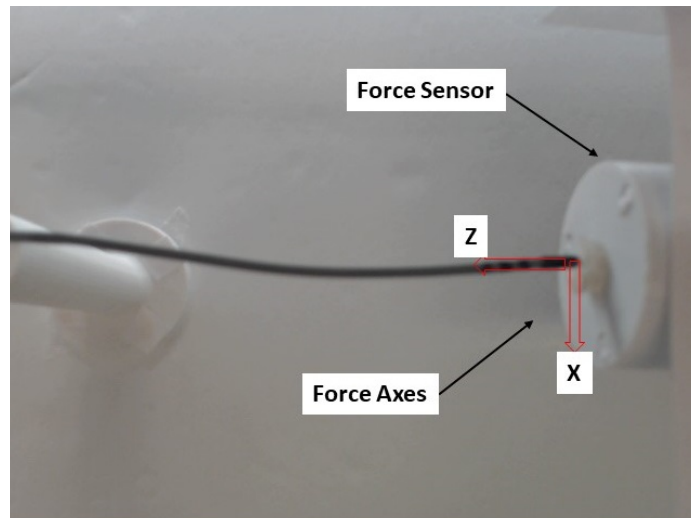
To actuate the system, a microcontroller (Arduino UNO) was used to send pulses commands to the stepper motor driver. An automation algorithm developed in Python sends the command to the microcontroller and also this program reads the measurements of the sensor and stores the images of the camera. In the following section, the details of the algorithm will be explained completely.



(a) Overall view of setup



(b) A view of Catheter, Sensor, Actuator and Camera



(c) The camera's image and force axes of the sensor

Figure 2.2: Uni-planar experimental setup

2.3.1 Automation algorithm

To arrange a dataset consisting of images and corresponding force data, an automation algorithm is necessary. The main goal of using this algorithm is to communicate between different components of the setup. This program was developed in Python language to send commands to the actuator and then to record the image of the camera alongside sensor readings. The final dataset including 2000 samples was stored in the computer for the next step of the research which is feature extraction and model training.

Figure.2.3 demonstrates the overall repetitive process of the data gathering and interaction between individual elements of the experimental system. After mechanical adjustments, and sensor and camera calibration, the Python program sends a manipulation command to the microcontroller to actuate the stepper motor for a predefined step. The microcontroller code was written in Arduino language and it transmits a pulse to the micro-step driver of the stepper motor. For this experimental study, the driver is set to 1600 pulse per revolution(0.2 rotational degrees per pulse) configuration to rotate the motor. After the rotation of the motor, an acknowledge signal should be sent to the computer program, indicating the successful rotation of the motor. This signal was sent after a time delay to make sure the vibrations of the rotation does not affect the force sensor reading. The next step is to capture an image from the camera and record the forces from the sensor. The image alongside its CF is stored in the computer. The described process will be repeated 2000 times to build the dataset.

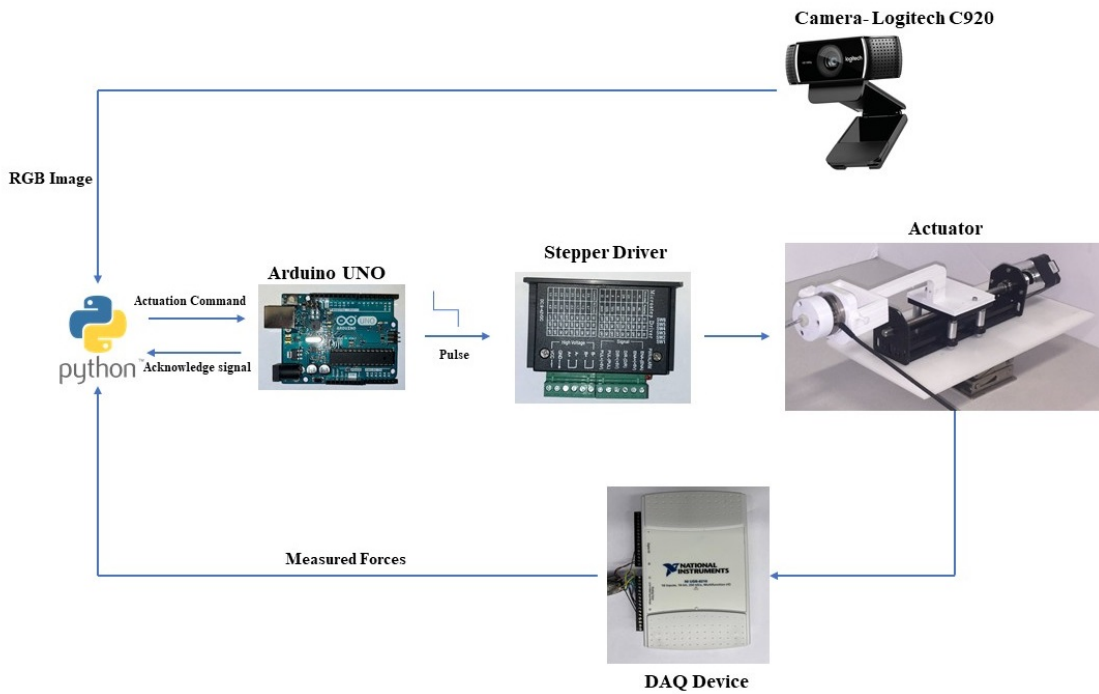


Figure 2.3: Software and hardware interaction of the setup for data acquisition

2.3.2 Vision system

The camera was used as a visual sensor to capture images from the distal shaft and then the image's data (pixels) will be used for the learning models. To have accurate and constant data, the relationship between 3D points in the real-world space and corresponding 2D projected pixels should be calculated. To this end, the internal and external parameters of the camera should be identified for calibration. Usually, internal parameters refer to focal length (f_x, f_y) and optical center (c_x, c_y) coordinates as shown in the following camera matrix. Accordingly, the external parameters are rotational and translational coefficients showing the orientation of the camera. By using a calibration pattern, the mentioned parameters can be found and the final image will be affected by the parameters. This process should be performed just once to make sure there is no distortion in the captured image.

A checkerboard pattern was fixed on a plate and some images from different orientations were captured. Afterward, as shown in Figure 2.4, corners of the checkerboard were extracted by using built-in functions of *OpenCV* (Open source computer vision library) in python language. By entering

the corner's locations into a calibration function, the parameters consisting of the camera matrix and distortion parameters were estimated. As the result, the extracted numerical values were used to make the image calibrated. Radial and tangential distortion are common issues in a raw image of the camera and to tackle these geometrical distortions, some coefficients are required to find the rate of distortions. Extracted parameters were used to make a normal image without distortion. The following are extracted parameters of the camera used for the setup:

$$\text{Camera matrix} = \begin{bmatrix} f_x & 0 & c_x \\ 0 & f_y & c_y \\ 0 & 0 & 1 \end{bmatrix} = \begin{bmatrix} 6.45E + 02 & 0.0 & 3.30E + 02 \\ 0.0 & 6.43E + 02 & 2.25E + 02 \\ 0.0 & 0.0 & 1.0 \end{bmatrix}$$

$$\text{Distortion Coefficient} = \begin{bmatrix} k_1 & k_2 & p_1 & p_2 & k_3 \end{bmatrix} = \begin{bmatrix} 3.72E - 02 & -8.11E - 03 & -4.27E - 03 & 7.51E - 04 & -2.72E - 01 \end{bmatrix}$$

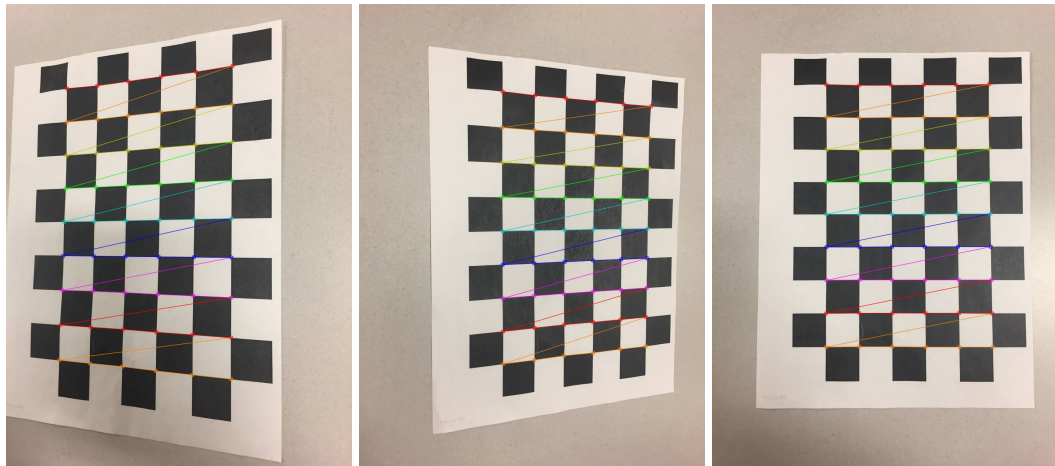


Figure 2.4: Chessboard calibration images

Rotation and translation vectors are external parameters that show the coordinates of a 3D object in the view of the camera. By using these parameters, the camera can be installed at a fixed location every time that data acquisition from the catheter is required. Due to the functionality of the image

extraction algorithm of the study which depends on the pixel's location on the body of the catheter, the location of the camera must be fixed for every run of data gathering and control loop experiments. The external parameters can be monitored by *calibrateCamera()* function in *OpenCV* and also another alternative is to use *Aruco* markers to identify the orientation of the camera as shown in Figure.2.5. The main reason for using these markers is to make sure the camera's lens surface is adjusted parallel to the curvature plane of the catheter.

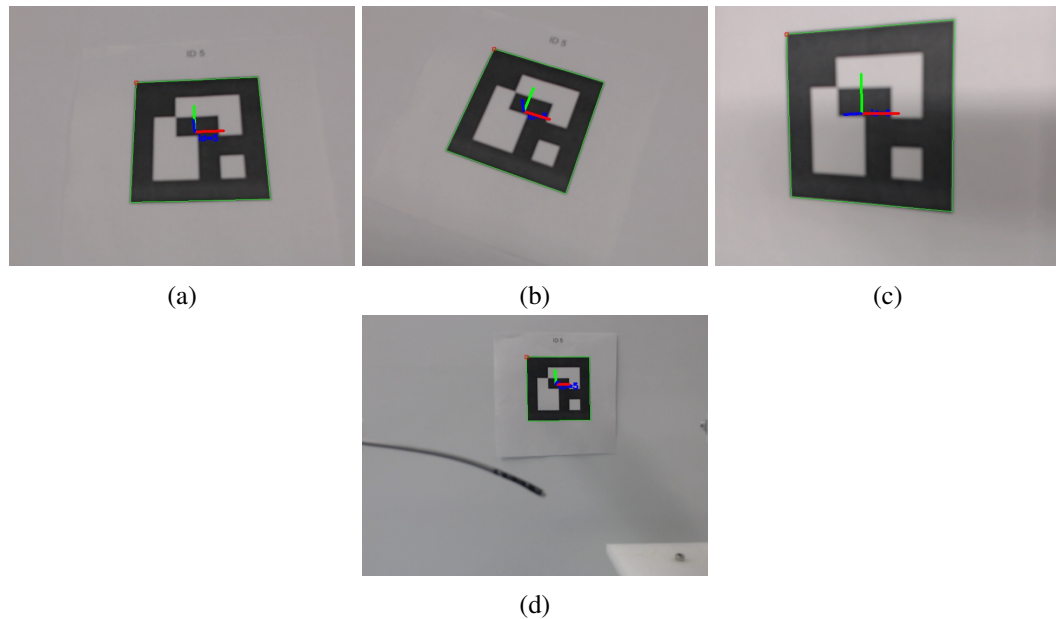


Figure 2.5: (a), (b), and (c) are Aruco markers in different orientation of camera - (d) is a view of the marker beside the catheter's distal shaft

2.3.3 Data

After adjusting the actuator and calibrating the camera, a dataset consisting of 2000 samples can be organized based on the described automation algorithm. As mentioned earlier the dataset is the combination of images and corresponding CFs from the distal shaft. Figure.2.6 illustrates some samples from the captured images and also Figure.2.7 depicts the CFs from the dataset. In this uni-planar experiment, just two CF components (x, y) were monitored and the CF orientations are visualized in Figure.2.2(c).

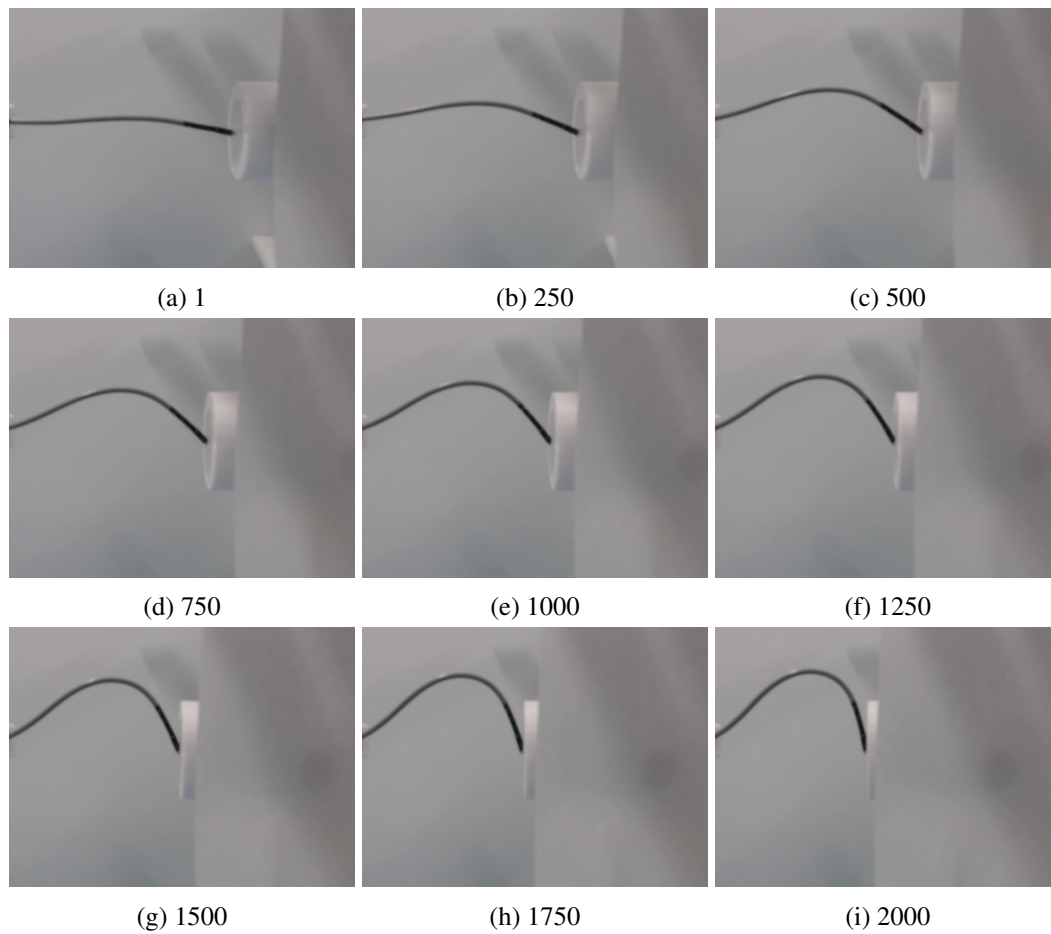


Figure 2.6: Images from the uni-planar dataset

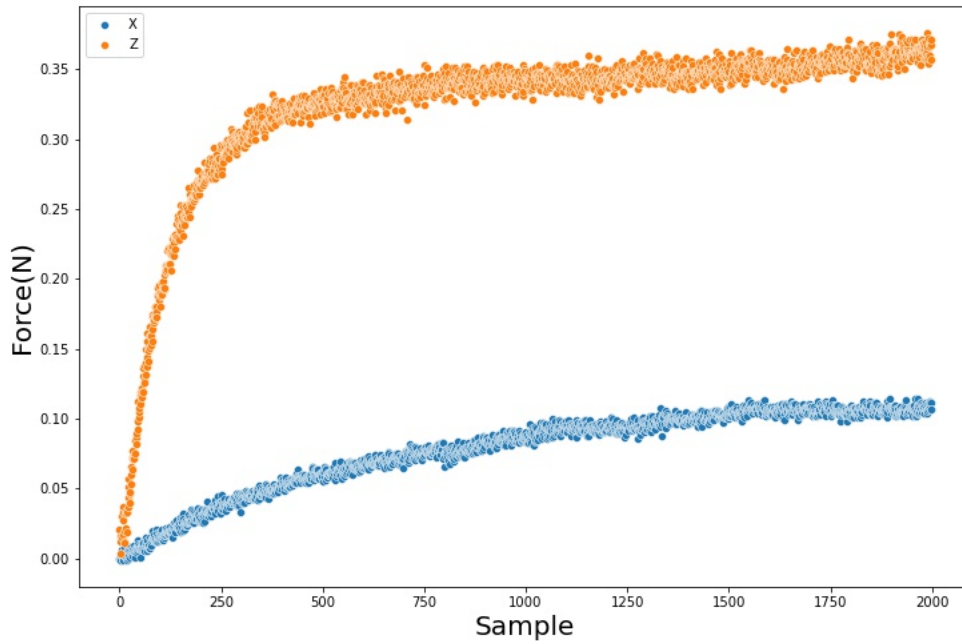


Figure 2.7: Force samples of the uni-planar setup

2.4 Catheter manipulator mechanism

The final goal of the present thesis is to propose a force controller that benefits from a vision-based force estimator as a force feedback element. In this regard, a catheter manipulator mechanism is required to hold the catheter and push the tip of catheter against the heart tissue. Figure.2.8 shows the designed 3-DoF electro-mechanical mechanism that is capable of insertion, rotation, and knob actuation of a standard ablation catheter. The mechanism was designed in *SolidWorks 2020* and fabricated by 3D printer using PLA material. This actuator was designed based on the basics of the commercially available robotic platforms described in section 1.1.4 in an attempt to be used for force control in Chapter 4. Two servo motors (Dynamixel XL430-W250) in a serial configuration were used for rotation of catheter's handle and actuation of the knob. For the insertion of the catheter, a DC motor(5840-31ZY, 130 RPM) was implemented to rotate the shaft of a linear stage actuator. The insertion was used for applying the force at the tip of catheter and more detail of the setup is

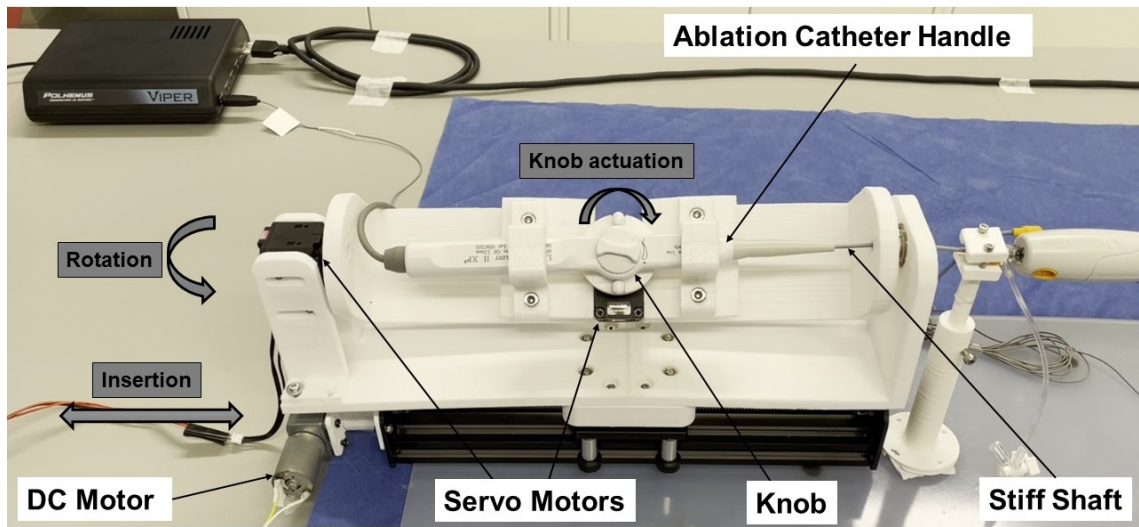


Figure 2.8: 3-DoF Catheter manipulator mechanism capable of insertion, rotation, and knob actuation

described in chapter 4.

2.5 Summary

In this chapter, firstly some available academic experimental setups for catheter ablation CF research were reviewed. Afterward, a uni-planar setup was designed and implemented to compile a dataset consisting of images of the distal shaft of the catheter under applied forces. The dataset is used in Chapter 3 to train machine learning models for CF estimation based on the image of the distal shaft. To use the CF estimator as the force feedback element of a control loop, a 3-DoF catheter manipulator was designed. This mechanism is used in Chapter 4 to maintain the CF at the desired value.

Chapter 3

A Vision-based Method For Estimating Contact Forces In Intracardiac Catheters

Atrial fibrillation is a kind of cardiac arrhythmia in which the electrical signals of the heart are uncoordinated. The prevalence of this disease is increasing globally and the curative treatment for this problem is catheter ablation therapy. The adequate contact force between the tip of a catheter and cardiac tissue significantly can increase the efficiency and sustainability of the mentioned treatment. To satisfy the need of cardiologists for haptic feedback during the surgery and increase the efficacy of ablation therapy, in this paper a sensor-free method is proposed in such a way that the system is able to estimate the force directly from image data. To this end, a mechanical setup is designed and implemented to imitate the real ablation procedure. A vision-based feature extraction algorithm is also proposed to obtain catheter's bending variations obtained from the setup. Using the extracted feature, machine learning algorithms are responsible of estimating the forces. The results revealed $MAE < 0.03$ and the proposed system is able to estimate the force precisely.

3.1 Introduction

Cardiovascular Diseases (CVDs) as one of the main reasons of global mortality are caused by disorders of the cardiovascular system [80]. According to heart disease statistics, the annual worldwide deaths associated with CVDs are over 17 million [1]. Atrial Fibrillation (AF) is a common heart arrhythmia which occurs due to erratic electrical impulse of the heart and has affected at least 3 to 6 million people in the United States [6].

Catheter ablation is a well-known minimally invasive treatment for AF to locally heat and destroy (ablate) arrhythmogenic cardiac tissue [81, 11, 12]. To perform the ablation treatment, a long flexible tube called catheter, is inserted into the vascular system to deliver some source of energy to the arrhythmia spots of the heart under X-ray fluoroscopy or MRI monitoring [13].

Adequate catheter-tissue Contact Force (CF) is known as a procedural success factor that leads to a sustainable effect of catheter therapy [42]. Accordingly, the force sensing system plays a significant role in cardiac catheterization [46]. In accordance with experimental studies, CF between $0.1N$ and $0.3N$ is a safe and effective range [39]. Besides, image-based position tracking of the catheter shaft and tip is considered as an important feature in terms of accuracy of guidance [82].

Sensor-based and sensor-free approaches are proposed methods for measuring the CF of a catheter's distal tip [47, 48]. Despite the fact that sensor-based methods are providing accurate measurement, implementation of tactile sensors in catheters has some challenges including high-end cost, physical issues ,and also difficulties in data acquisition systems in the unstructured environment [49]. Accordingly, as an alternative, sensor-free methods have caught attentions in the literature [47].

One approach of the sensor-free method is the analysis of catheter shape in which a parameter called "force index" is identified to address the force range [61]. However, based on experimental results, this method is not capable of detecting the full range of forces. Another approach is model-based techniques consisting of beam theory models, Cosserat-type rod theories ,and multi-body dynamics [60, 83, 84]. Although the mentioned model-based manners in some cases provide an accurate estimation of the force, the main effective factor for this accuracy is the optimal model parameters [69]. In another study, Runge *et al.* [70], used a finite element model to train an artificial

neural network for soft robotic application. However, this method requires accurate finite element modeling in which the material parameters and manufacturing aspects of the soft robot should be considered carefully.

Overall, the accuracy of the model-based methods highly depends on the model parameters. In addition, they are computationally expensive, especially when it comes to detection of a real catheter from the operating room's monitor as these models need information from the image of the catheter.

In this study, we proposed a new vision-based solution in collaboration with machine learning methods to address the CF issue in ablation catheters. This system is functional as a sensor-free and real-time method in which the CF can be estimated directly from the image data. As the deflectable distal shaft of the catheter has unique bending under applied forces, this behaviour can be considered as a distinguishable factor of force estimation [61]. Accordingly, in this work, a mechanical setup has been designed and implemented in order to simulate the authentic Operation Room (OR) along with the available tools for performing an ablation task. Using the data captured from the aforementioned setup, a machine vision algorithm is devised as a feature extractor to find the points on the catheter's deflectable distal shaft within images. These points are deemed as the features which translate the catheter's tip into a numerical feature space. Subsequently, multiple architectures for Artificial Neural Networks (ANN) have been designed and implemented so as to model the extracted features and map every catheter's image to its corresponding contact force. In addition to ANNs, we model the data using Support Vector Regression (SVR) with the aim of making a benchmark. These models are considered as a system which maps the features to the CF in x and y direction. In the next section, the developed experimental setup and data compilation will be explained. Then, the methodology including the feature extraction algorithm as well as the modeling methods will be elaborated. The paper will be concluded in the last section.

3.2 Experimental setup and procedure

The experimental setup used for data collection is shown in Fig. 3.1. In this setup, the camera plays the role of X-ray fluoroscopy machine in a real OR. In addition, a motorized linear actuator

simulates the heart motion (one direction) in which an attached force sensor is recording the CF.

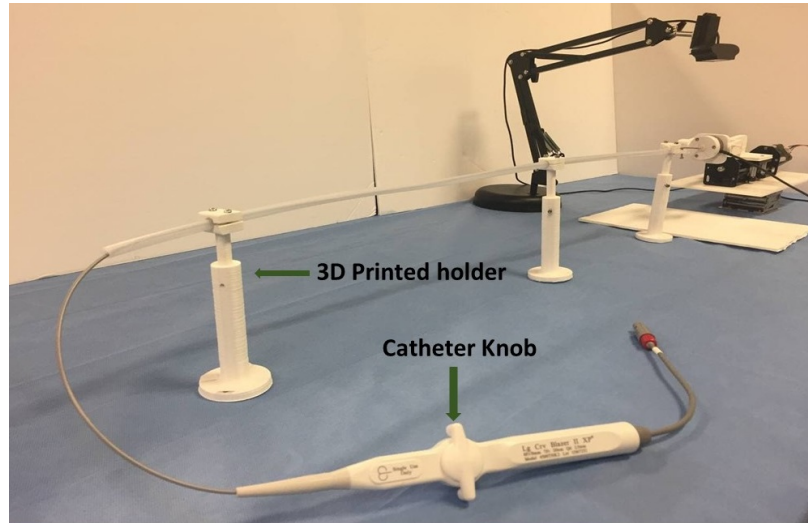
3.2.1 Experimental setup design

The experimental setup is designed in an attempt to collect images from the deflectable shaft of the catheter and corresponding forces. Fig. 3.1 presents the setup consisting of a 1-DOF (Degree Of Freedom) linear actuator equipped with a 2-phase stepper motor (17HS4401-S 40mm Nema) powered by a micro-step driver (HANPOSE TB660), a Camera (C920 for 640×480 pixels resolution), a 6-DOF Force sensor (ATI Mini40), a Bi-directional catheter (Boston Scientific Blazer II XP), 3D printed parts for holders and a plastic sheath. In this setup, the catheter is passed through a plastic sheath in a straight path in which the sheath is fixed by 3 holders and the Knob of the catheter is configured at zero degrees. The deflectable section at its base point where the body of the catheter is connected to the bending section is fixed by the 3rd holder. Hence, it cannot move inside the sheath. The force sensor attached to the 1-DOF motorized actuator is used to measure the applied forces at the tip of the catheter. In addition, the camera is implemented perpendicular to the bending section to capture a planar image for every sample.

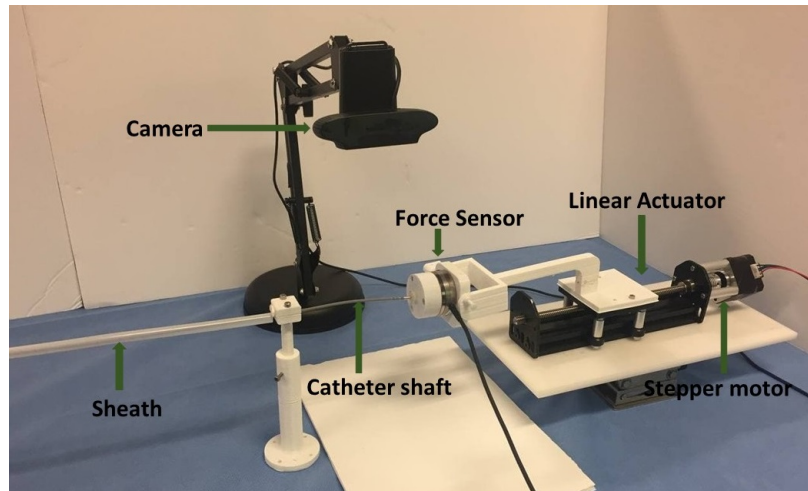
3.2.2 Data Collection

Fig. 3.2 depicts the interaction between the software and the hardware in the experimental setup to collect a dataset comprising of 2000 sample images from deflected shaft under the applied forces by the actuator. After calibration of the sensor, data collection is done by following steps for each sample:

- (1) A Computer program developed in Python sends a command to an Arduino UNO to manipulate the motorized linear actuator.
- (2) The Arduino and stepper motor driver control the stepper motor rotation for three micro-steps equivalent to 0.6 degree (the driver is set to 1600 pulse per revolution to reach 0.2 degree per pulse).
- (3) Afterward, the Arduino sends an acknowledge signal to the computer.



(a) Overall view of setup



(b) A view of Catheter, Sensor, Actuator and Camera

Figure 3.1: Experimental Setup

- (4) The image of the deflected shaft of the catheter is captured.
- (5) The force data (two directions) is recorded from a 16-bit data acquisition device (USB 6210, National Instruments, Austin, TX).

This procedure is repeated 2000 times to build a dataset that contains deflected shaft images from the initial shape of the bendable shaft to fully deflected formation and their corresponding forces.

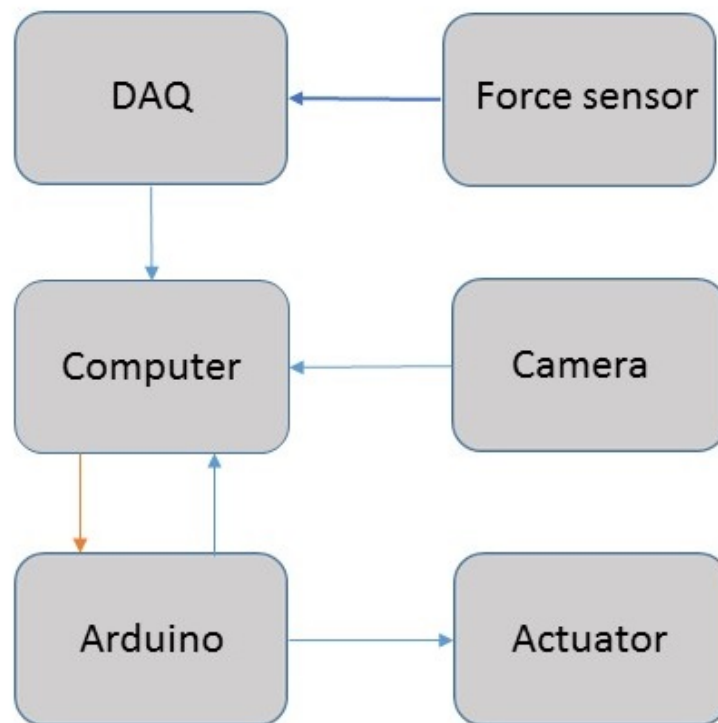


Figure 3.2: Software and hardware interaction

3.3 Methodology

3.3.1 Feature extraction

Monitoring the catheter's deflection (distal shaft) during the ablation process provides information about CF [61]. In this regard, a real-time machine vision algorithm is required to extract features and translate the deflection in a numerical feature space. In this study, we have proposed an algorithm to obtain ordered points as features on the body of the catheter's deflectable section. The **Algorithm 1** shows the image processing procedure to extract ordered points from the base point of the deflectable shaft to the tip of catheter. An image captured by the camera is presented in Fig. (3.3a). This image is converted to the gray scale format and then a binary threshold operation is applied to segment the catheter in the image [see Fig. (3.3b)]. Subsequently, the algorithm vertically searches through the matrix of the 2D binary image until it finds the body of the catheter. At this point, the Cartesian coordinates (x and y) are stored as the first feature. This procedure continues until the last possible vertical search path is met. The distance between each vertical search path is a hyper-parameter that defined as the skip point. This criteria denotes the number of features. For instance, every image is represented in a 106-dimension feature space, if the skip point is equal to 5. Fig. (3.3c) depicts the overall procedure of vertical search where blue lines indicate the search path. Fig.(3.3d) shows the extracted ordered points (features) on the catheter in which the tip as the last recorded point is detected.

The aforementioned algorithm is applied to 2000 images and multiple datasets have been generated with different values for the skip point. Using the compiled datasets, the machine learning models are responsible of estimating the forces.

3.3.2 Machine Learning Models

Having the output data of the feature extraction phase, a modeling method is required in between so as to map every single record of the dataset to its corresponding force value. Since the goal is to estimate the forces directly from the images, the modeling technique deals with continuous values. In contrast to the modeling of quantitative values as a classification problem, in the current work, the system strives to create a regression over the data. With this in mind, two more popular modeling

Algorithm 1 Feature Extraction Algorithm

Input:RGB image from the Camera

Output:Ordered points on the body of catheter

GrayscaleFunction(RGBimage)

ThresholdFunction(Grayimage)

Flag =False

j=0

for $i = 0; i \leq width; i = i + 5$ **do**

for $j; j \leq height; j + = 1$ **do** Flag =False
 pixel location=[i,j]

 pixel value ==0 Record i,j location of the point

 Flag=True

 j=horizontal location of the point+30

 Break the Vertical(height)search loop

 Continue the Vertical(height) search

 Flag==False Break the Horizontal(width) step loop

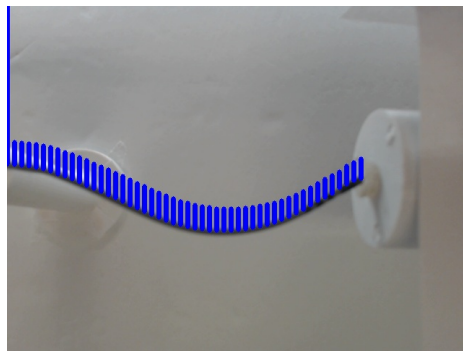
 Continue the Horizontal(width) search



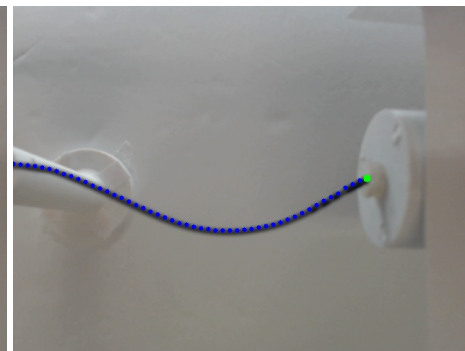
(a) Original Image



(b) Binary Image



(c) Search Path



(d) Points

Figure 3.3: Features Extraction

approaches have been intended with multiple configurations in order to approximate the forces in x and y direction: Artificial Neural Network (ANN) and Support Vector Regression (SVR) [85, 86].

The ANN is considered to receive a feature vector $x \in R^m$ where m is the number of features depending on the the settings of the feature extraction phase. It is also expected to output the result in a two-dimensional space in order to estimate the actual forces in x and y direction. To this end, a combination of the following stacked layers is deemed so as to design the architecture of the ANN. The input feature vector x goes into a dense layer:

$$n_l = \sigma(W_l n_{l-1} + b_l) \quad (3)$$

Where W and b are the weights and biases (neurons) respectively. l denotes the layer of the network and n_l is the output of the current layer l . In addition, n_{l-1} indicates the output of the previous layer while for the first layer $n_{l-1} = x$. Also, σ is the activation function in such a way that for the intended architecture the *ReLU* is preferred:

$$\sigma(z) = \max(0, z) \quad (4)$$

Obviously, the activation function above squeezes the negative value and replace them with 0. Moreover, it is common in the Deep Learning (DL) and ANN to equip the model with the regularization term, e.g., "L1 or L2-Regularization" with the aim of preventing the model from over-fitting. Here in this design, the Dropout is opted as the alternative to the regularization method above. In this method, a coefficient δ is multiplied by every component of the W and b matrices and calculated as follows [87]:

$$\delta = \begin{cases} w_j, b_j & \text{with } P(r), \\ 0 & \text{otherwise} \end{cases} \quad (5)$$

In fact, the component j of the parameter matrix W or b is remained with the probability $P(r)$ where $P \sim \text{Bernoulli}(r)$ and in this architecture $r = 0.1$. It is worth noting that, Batch Normalization (BN) method is widely used in ANN in order to accelerate the optimization process [88]. In this

Table 3.1: The performance of multiple modeling methods with different configurations.

No.	method	configuration	layers	feature dim	skip points	MAE	MSE	R2
1	DNN	dense	9 layers	36	15	0.023	3.4868e-04	0.984
2	ANN	dense	[128, 64, 2]	36	15	0.021	3.5274e-04	0.986
3	ANN	dense	[128, 64, 2]	106	5	0.020	4.4928e-04	0.978
4	ANN	dense	[128, 64, 2]	22	24	0.023	3.0972e-04	0.986
5	ANN	dense + dropout	[128, 64, 2]	36	15	0.0401	0.0515	0.218
6	ANN	dense + batch	[128, 64, 2]	36	15	0.023	5.0931e-04	0.974
7	ANN	dense + batch + dropout	[128, 64, 2]	36	15	0.0345	0.022	0.328
8	SVR	linear	-	22	24	0.025	3.0705e-03	0.913
9	SVR	linear	-	36	15	0.028	1.9133e-03	0.9449
10	SVR	linear	-	106	5	0.024	6.2738e-04	0.982

work, the design incorporates the BN to the graph prior to applying the activation function. The last layer of the network outputs a vector with two elements corresponding to x and y forces. To optimize the model and train the neurons, Mean Absolute Error (MAE) is selected as the loss function of the model:

$$MAE(n_l, f) = \frac{\sum_{i=1}^n |n_{l,i} - f_i|}{n} \quad (6)$$

In the equation above, f denotes the actual forces that the model is supposed to estimate. The designed network can be optimized using Adam optimizer [89].

For the sake of benchmarking the eclectic number of modeling methods for the regression problem upon the extracted features, a linear Support Vector Regression (SVR) has been utilized in order to generate the forces out of the the given features [86]. Since the SVR is a well-known traditional Machine Learning (ML) algorithm for which it has widely contributed to a broad range of applications and also there are valuable references in the literature about it, in this work, we will not explain the method in details. Two separate SVR models are considered for this problem: the SVR for the force in x direction and the other one for y direction. It is worth to say that, the ANN and all derived

configurations have been implemented on Python using Tensorflow 2.4 while the implemented API of Sklearn has been utilized for the SVR models [90, 91]. In contrast to the ANN models, no further modification or implementations have been done for the SVR models.

3.4 Results and Discussion

In this section, the performance of the proposed system has been investigated in both the feature extraction and the modelling phase. To this end, a diverse range of configurations has been designed and the results have been compared using three main metrics: MAE, MSE and R2. The feature extraction module was fed by a dataset containing 2000 images of the catheter's tip. The dataset obtained from the feature extraction phase was normalized and divided into three sub-datasets: a training set encompassing 1280 samples, a testing set containing 400 samples and a validation including 320 samples. As reported in Table 3.1, 10 different configurations have been design so as to compare the performance of the proposed method accurately. For all NN-based methods every batch of the dataset includes 16 samples and the system was trained in 200 epochs while the learning rate $lr = 0.001$. The first configuration is a graph of 9 dense layers as a feed-forward NN in which the layers contains the following neurons respectively: 256, 256, 128, 128, 64, 64, 32, 32, 2. This model trained on the dataset comprising 36 features acquired from the feature extraction algorithm with 15 skip points. The second configuration has a shallow architecture while the layers are analogous to the previous Deep NN in terms of layer's type. This NN showed a better accuracy whereas the parameters was considerably decreased. One reason is that the complexity of the captured data was not significant so a shallow NN was capable of extracting the model properly. However, the deeper network needs more epochs to be trained completely.

Configuration 2 to 4 investigated the impact of feature extraction phase and the feature dimension in the modeling. As it can be seen, given the fact that the training epochs was the same for all configurations, the representation of the catheter images in higher dimensions did not reached to an acceptable performance. However, the data with more features not only needs more parameter and epochs to be trained but also it requires a deeper NN to obtain the relationship between every dimension. Configuration 5 to 7 inspected the influence of adding batch normalization and dropout to

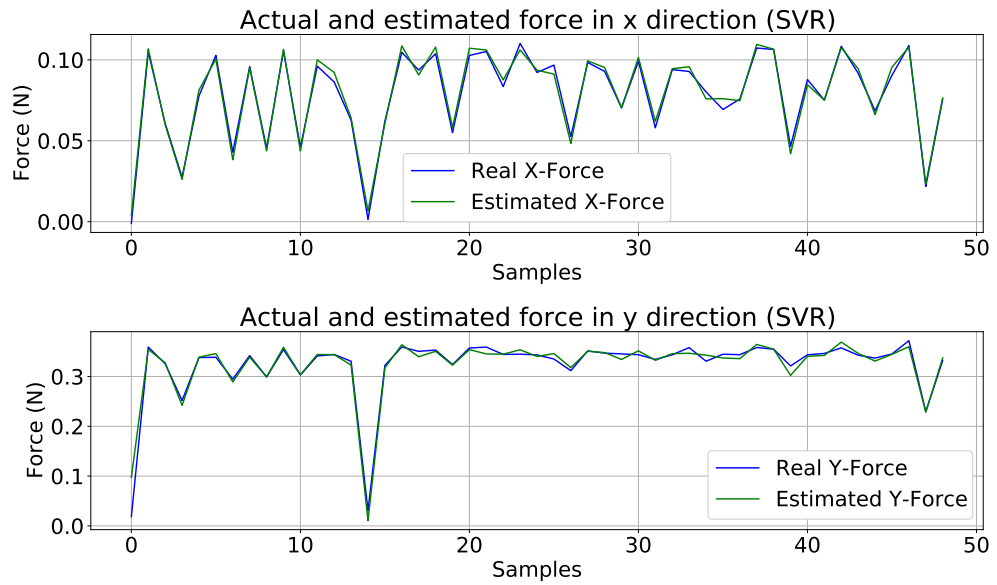


Figure 3.4: The performance of the SVR for approximating the forces in both x and y direction.

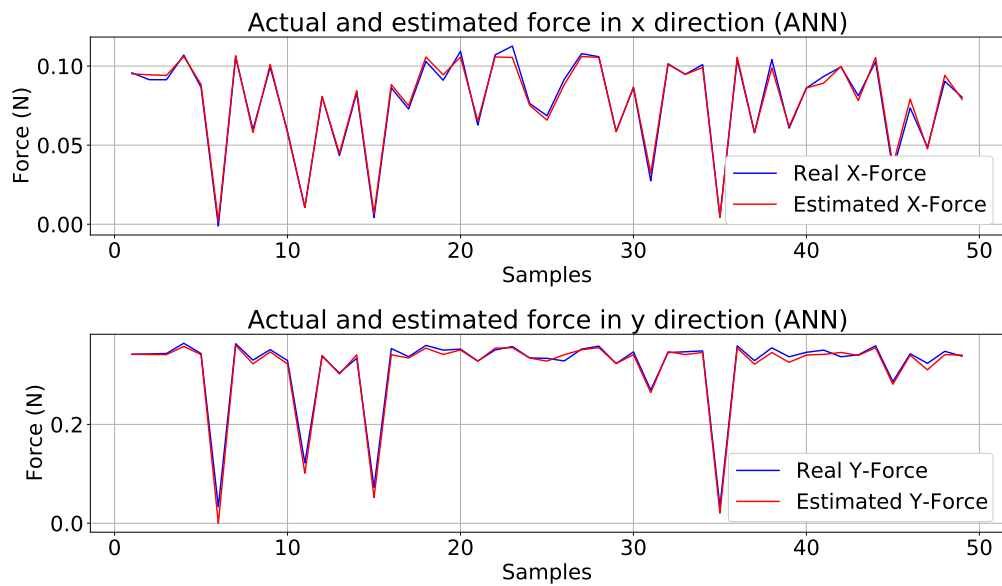


Figure 3.5: This plot shows the performance of the designed ANN in estimating the forces in x and y direction.

the network's graph. The dropout layer prevent the model from reaching to the convergence point. It is worth noting that, the training loss was tracked on the validation set during the training phase and no evidence of over-fitting was caught.

The last three configurations in Table 3.1 reported the performance of a linear SVR model on the datasets. For every dataset, two separate SVR models were trained: one for the estimation of forces in x direction and the other one for y direction. The reported results are the average of corresponding metrics for x and y models. The tolerance for stopping the training procedure was set to 0.001. Given the tolerance value, the system keeps learning until the tolerance becomes satisfied. For this reason, the impact of representing data in different dimension size can be tangibly evaluated. The SVR showed a better regression's performance on the dataset with higher dimensions while the over performance of the ANN methods surpassed. Fig.3.4 and 3.5 demonstrate the performance of configuration 2 and 10 respectively and show the proposed system can estimate the actual forces accurately.

3.5 Conclusions

In this work, a sensor-free method has been proposed for estimating the force of the catheters' tip with the aim of contributing to the catheter ablation treatment. The method is capable of approximating the forces directly from the images. To this end, a mechanical setup has been designed and implemented in order to imitate an authentic operation room for catheter ablation. Using the setup, the system compiled a dataset containing the images of a catheter's tip and the forces associated to every image. A feature extraction algorithm has been proposed to extract the variation of catheter's deflection within the images and represent them in the multi-dimensional feature space. Having the dataset of extracted features, different feed-forward neural network has been designed and implemented to make a regression over the data. Besides, Support Vector Regression as a conventional machine learning method was deployed to model the data as well. The output of the proposed feature extraction collaborating with the implemented modeling methods estimated the forces precisely. As the future work, we will extend the current system in such a way that the 3D forces can be estimated directly from the images without a feature extraction phase.

Chapter 4

Force control on intracardiac catheters through adaptive monoplanar imaging and neural force estimation

Catheter-tissue contact force(CF) has been reported as one of the success factors of heart ablation surgery. Monitoring and controlling the CF are challenging processes due to the limitation of sensing technologies and robotic surgery systems. In the present study, an image-based and sensorless CF controller system is proposed that is capable of maintaining the desired CF. A real-time and accurate force feedback element was designed and evaluated to estimate the CF directly from the image of the ablation catheter's deflections during the surgery. This estimator is consisting of an image-based feature extractor and an artificial neural network model. The neural estimator successfully could provide CF with a mean absolute error of 0.012 ± 0.01 N. This estimator element was implemented in a closed-loop CF controller to apply the required force to the heart tissue to perform the ablation treatment for heart beating abnormality. An experimental setup including the ablation catheter manipulator mechanism and a robotic camera localization system was designed to evaluate the performance of the CF controller for static and dynamic input CFs. The designed manipulator was deployed to achieve the desired CF and a robotic arm was used to track the catheter's bending section to be used for the feedback element of the controller. The evaluation tests showed that the

system can maintain the CF with root-mean-squared(RMS) error of $0.01 \pm 0.01 N$ for static test and RMS error of $0.04 \pm 0.03 N$ for dynamic input forces.

4.1 Introduction

4.1.1 Background

Radio-frequency ablation procedure known as the effective treatment of the choice for atrial fibrillation heart disorder [92], [93]. In this cardiac failure, the heart beats irregularly due to uncoordinated electrical distribution in some spots of the heart muscle. During ablation treatment as minimally invasive surgery, the cardiovascular interventionist inserts a flexible hollow shaft, named steerable sheath into the cardiac system of the body, usually from the femoral vein of the leg to reach the heart chamber. Then, an ablation catheter should be advanced to the sheath in order to destroy the target area commonly by heating generated by radio frequency power source [14]. As shown in Figure.4.1, The ablation catheter is a wire-like steerable surgical tool that an electrode is embedded at its tip to deliver radio frequency energy to the abnormal spots of the heart for ablation.

The catheter-tissue contact force(CF) plays an important role in terms of effectiveness and sustainability of the treatment [42], [46]. According to clinical studies, CF between $0.1N$ and $0.3N$ is a desirable range in such a way that excessive CF may lead to heart tissue damage, and on the other hand, insufficient CF results in poor efficacy [39], [94]. CF measurement methods fall into two categories including sensor-based and sensor-free approaches to monitor the CF for the surgeon [19]. In the sensor-based method, the catheter is equipped with a tiny force sensor at the tip, and supporting devices display the force magnitude [10], [95]. In contrast, the sensor-less strategy is based on mathematical and dynamic analysis of the catheter behavior to estimate the CF [19].

TactiCath catheter developed by *St Jude Medical*, *THERMOCOOL SMARTTOUCH* by *Biosense Webster* and *DIRECTSENSE* technology by *Boston Scientific* are the well-known sensor-based systems that they provide CF and sensing information by using custom-designed catheters. However, these systems are costly, and considering the fact that catheters usually are disposable, makes these sensing technologies expensive [19], [49]. Recently sensor-less or model-based methods have

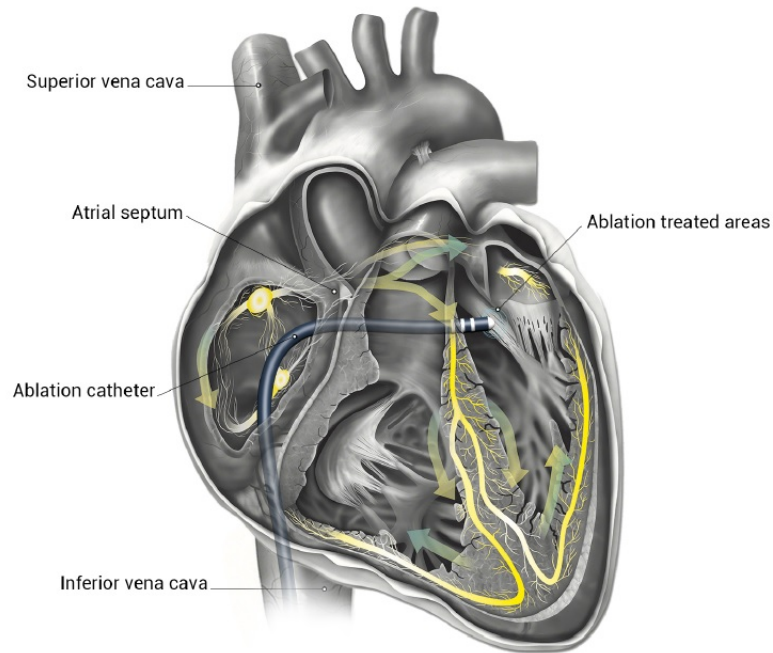


Figure 4.1: Ablation catheters inside the heart chamber[96]

demonstrated the promising results in CF estimation by conventional catheters [97], [67]. Mechanical or learning models have been developed to report the CF commonly based on the bending of the catheter's distal shaft which is the more deformable segment of the catheter. Among the sensor-free approaches, the learning method has caught attention in the literature due to the benefits of this modeling manner. Mechanical modeling requires considerable complex analysis of the mechanistic behavior of the distal shaft as a soft robot and also the accurate model's parameter identification still is challenging [69]. Although the model-based technique provides CF information in some cases, the machine learning methodology overcomes the mentioned concerns of mechanical modeling.

Machine learning techniques use the actual catheter's features such as images of the deflected distal shaft under corresponding applied forces to train a model to be used for CF estimation. In this method, the input of the trained model can be an X-ray image of a real-time fluoroscopy machine from the catheter during the surgery and the output is the applied force in a commonly used ablation catheter. This intelligent vision-based system enables the surgeon to monitor the CF information on a display or the force can be provided as haptic feedback to mimic the sense of touch during the treatment.

Despite the fact that providing real-time CF data effectively increases the success rate of surgery [98], [99], the sustainable control of the CF at the desired level is a significant parameter. During the ablation procedure, an internationalist applies an adequate force to the target spot but because of the sinusoidal beating of the heart tissue, the compensation of the force is a challenging process. Furthermore, as the surgery should be done under X-ray exposure, both surgeon and patient are under harmful radiation risks [100]. In accordance with mentioned clinical needs, studies show that implementation of CF technologies not only improves the outcome of the surgery but also considerably reduces the procedure and X-ray exposure duration[43].

4.1.2 Related studies

In an attempt to design a force control system, a CF estimator or sensing technology is an essential element. As mentioned earlier, sensor-less estimators show superiority in terms of CF measurement. In this regard, recently implementation of machine learning(ML) approaches resulted in accurate and fast enough CF estimation.

In one study, Nourani *et al.*[74] considered the distal shaft of an ablation catheter as a polynomial curve and coefficients of the polynomial were extracted as the input of a ML model to estimate the CF. However, as this image-based method requires many preprocessing steps, it is not ideal for real-time CF controllers. In another study, Sayadi *et al.*[73] proposed a learning-from-simulation method to estimate CF based on features that are extracted from the images of a finite element simulation of the catheter under a range of applied forces. Despite the accurate estimation of the trained models in this research, validation of the simulation and also parameter identification are the main limitations.

To use a ML model as a feedback element in a control loop of CF, a real-time and precise vision-based model is required. In accordance with the aforesaid criteria, in this paper, a vision-based technique has been implemented that was proposed by the author in [101]. The proposed estimator is a trained artificial neural network(ANN) model that the input is the location of pixels on the body of the distal shaft and the output is the CF information. A dataset consisting of the catheter's images under a range of applied forces was arranged and a feature extractor algorithm finds the required pixels for every captured image. The result showed that the CF was reported with mean absolute error(MAE) of $0.04 \pm 0.02N$ and root mean square(RMS) error of $0.01 \pm 0.02 N$

which according to clinical studies is an acceptable error rate. More considerably, this method takes 0.007 seconds per video frame to provide the CF which is an ideal estimator element for a real-time control system. The frame-per-second rate of X-ray fluoroscopy machines is about $30Hz$.

To design a control system for CF on a beating tissue, Kesner. *et al.*[102] introduced a system consisting of a 3D-printed force sensor mechanism that is attached to the tip of a catheter. The system can achieve the CF at the desired level with an RMS-error of $0.11N$ which is not accurate enough for the ablation procedure. In other work, a soft miniaturized actuator with force sensing units was designed for the tip of the ablation catheter to control the CF[103]. Although the system controls the force quickly, the usage of customized actuation and sensing units is the main limitation and it cannot be used for commonly used catheters. In the area of sensor-based CF control research, Gelman. *et al.*[104] proposed and evaluated a hybrid PID controller for CF in ablation catheters during dynamic beatings of the heart. The controller is functional in a real-time manner with an RMS error of $0.03 \pm 0.007N$ but this system relies on the usage of catheters with embedded force sensors. To control the CF without a sensor, vision-based systems are the most favorable schema in the literature. Researchers in [105], evaluated a sensor-free force control approach that benefits from the vision feedback element through a position-based estimator modeling. However, the parameter identification of the proposed mathematical contact model and the lack of an image segmentation algorithm are notable issues of the system.

To overcome limitations of estimators and control systems, in this article a model-free control system with ML estimator as a feedback element is introduced. This system is functional for commercially available catheters and can maintain the CF at the desired value for quick beatings of heart tissue. A ML model was trained by a dataset consisting of 2000 samples to be part of the feedback element of the control loop and the proposed vision-based controller is capable of rapid and precise actuation. An actuator mechanism was designed to maneuver the ablation catheter for CF control. A camera was used to imitate the x-ray fluoroscopy imaging system and also a robotic arm was deployed to hold the camera at a fixed location and position. The camera constantly captures a fixed view of the distal shaft during the procedure and it rotates around the distal shaft depending on the rotation of the catheter's actuator mechanism.

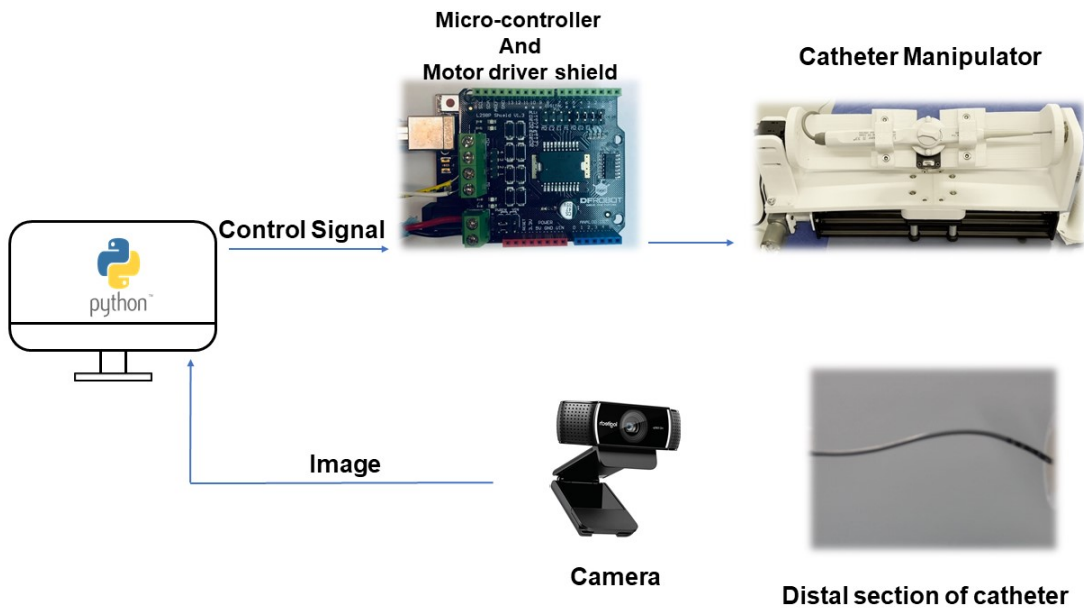


Figure 4.2: Overview of the system

4.1.3 Contributions

Following, the main contributions of this paper are listed:

- (1) Proposing a sensor-free and vision-based method for estimating CF in ablation catheters
- (2) Designing an adaptive vision system to track the catheter's distal shaft
- (3) Proposing a fast and accurate model-free control system for CF of ablation catheters

In Section 4.2, the proposed CF estimator, controller system schema and experimental setup are described. Section 4.3 provides the evaluation studies to discuss the performance of the system. In the end, section 4.4 concludes the study.

4.2 Methodology

In this section, an overview of the CF controller system is provided. Firstly, the overall framework of the system is introduced and also the neural force estimator including the feature extractor and ANN model is described in detail. Afterward, the sensor-free control loop schema is proposed.

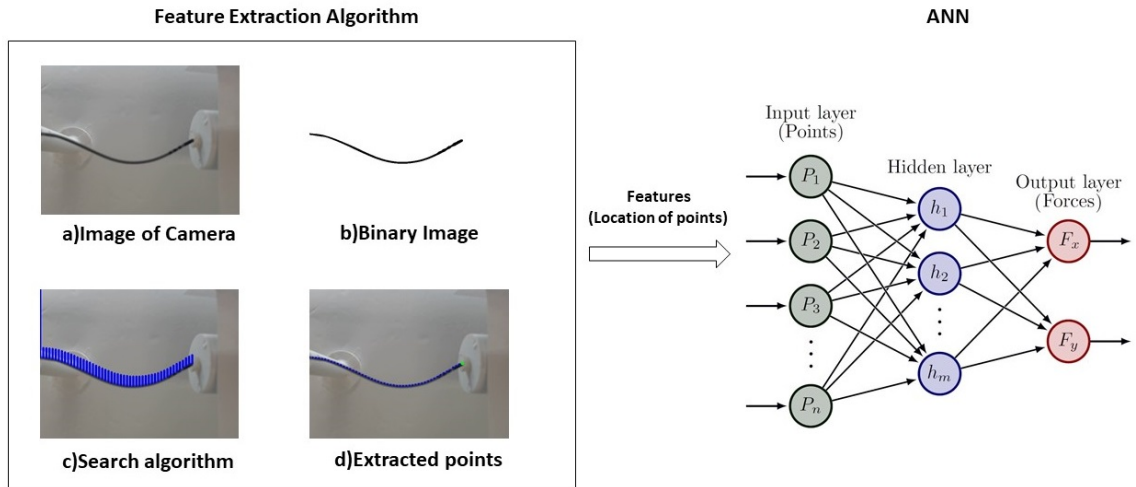


Figure 4.3: Proposed neural CF estimator

Finally, the experimental setup for data collection of ANN and the catheter manipulator mechanism for CF control are described.

4.2.1 Force control framework

The overall view of the CF controller system consisting of software and hardware parts is represented in Figure.4.2. A 3 Degree-of-Freedom(DoF) catheter manipulator was designed to advance the catheter to apply the force on the cardiac tissue which was controlled by a Micro-controller. The robotic vision system was deployed to capture images of the distal section of the catheter and send them to the computer for CF estimation. The Computer program developed in Python directly receives images and feeds them to the CF estimator to be used as the feedback element of the control loop. To actuate the 3 DoF catheter manipulator, control signals were sent to the micro-controller from the Python program of the computer through serial communication.

4.2.2 Neural force estimation

Figure.4.3 demonstrates the CF estimator structure which is based on the previous study of the author[101]. The deflection of the distal shaft during ablation is a useful indicator of applied CF. In this regard, the feature extraction algorithm is based on the coordinates of pixels on the

body of the distal shaft. The distal shaft in the view of the camera was segmented by deploying a binary threshold operation and then a pixel-wise algorithm was deployed to find the pixels on the curved shaft. The coordinates of detected pixels were based on a vertical search that starts from the origin of the binary image and it goes pixel by pixel to find the first point on the body of the distal shaft. This vertical search continues to find the last point which is located at the tip of the catheter and the distance between the vertical search is a hyper-parameter that is called the skip point. This algorithm was applied to all 2000 images of the dataset to build a new numerical dataset for ML training. Having a small distance for the skip point makes the algorithm computationally slow but in contrast, the long skip point distance results in insufficient points for the ANN model. Based on experiments, the skip point of 10 pixels was chosen for the horizontal distance of search columns and also the start point of each column was based on the last detected point's coordinates. In other words, the new vertical search column does not need to start from the top of the 2D matrix of the binary image. As the result of the aforementioned modifications, the algorithm is capable of extracting features for 0.007 seconds per video frame which makes it ideal for real-time applications. The algorithm was deployed on Python using OpenCV 4.6.

As shown in Figure.4.3, a three-layer feed-forward neural network was used to train a model to map the points from the feature extraction algorithm to corresponding forces. Regarding the promising performance of this ANN configuration in the previous study, the present ANN structure is proposed for CF estimation with slight modifications[101]. This network has 48 input neurons that are fully coupled with a feature extraction algorithm, an output layer with two neurons(F_x , F_y), and a single hidden layer. Also, the rectified linear unit(*ReLU*) was chosen as the activation function of the proposed ANN and *Adam* optimizer was deployed for compiling the model. The numerical dataset randomly was split into 1280 training data, 400 test data, and 320 validation data. The training data was normalized to scale the dataset and also to prevent over-fitting, the *EarlyStopping* callback method was deployed. The callback method stops the learning process once the loss between the training and validation set reached the minimum value of mean square error as the loss function. The proposed ANN was implemented in Python using Tensorflow 2.3.

$$INPUT\ of\ ANN = \left\{ \begin{array}{c} P_1 \\ P_2 \\ \cdot \\ \cdot \\ \cdot \\ P_n \end{array} \right\}, \quad OUTPUT = (F_x, F_y)$$

4.2.3 Controller design

After training the proposed ML model, it was saved to be used directly as the feedback element of a closed-loop control system. This model-free system benefits from the fast and accurate estimation of the CF that the feedback block just takes 0.01 seconds per video frame to estimate the applied CF from the camera. As illustrated in Figure.4.4, a proportional-derivative (PD) controller was used to minimize the error($e(t)$) between the desired and estimated CF, F_D and F_{SC} , respectively. The output control signal was limited between 0 and 255 as a PWM signal to run the DC motor of the 3-DOF catheter manipulator mechanism that inserts the catheter. The PD controller was deployed in the Python program in a computer and it sends output signals every 100 milliseconds to the micro-controller (Arduino UNO) over serial communication. Then the micro-controller sends PWM signals to the motor driver for actuation. The controller's gains(k_p and k_d) were tuned manually for a fast and constant CF control.

$$e(t) = F_D - F_{SC} \quad (7)$$

$$Control\ signal = K_p e(t) + K_d \frac{d}{dt} e(t) \quad (8)$$

4.2.4 Experimental setup

An experimental setup for both data collection and CF control was designed. The first system was used for data acquisition in which a linear actuator moves forward for a defined range. For every actuation, the image of the catheter bending section and its corresponding force data were

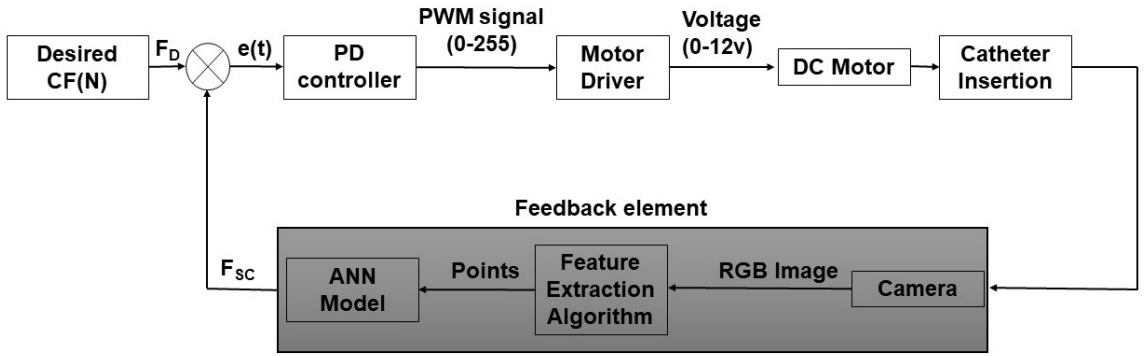


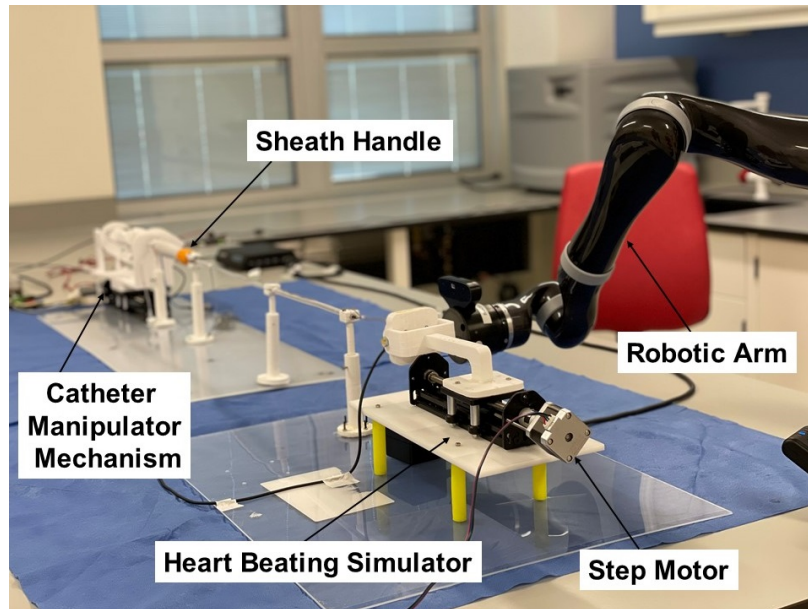
Figure 4.4: controller

recorded. This process was repeated 2000 times to compile a dataset of images and forces. This dataset was used for feature extraction and training of the ANN model. Due to the nature of the vision-enabled estimator that is based on the coordinates of pixels on the body of the distal shaft, the location of the camera during the CF controller functionality must be similar to what it was in the data collection phase. In the present article, to overcome this issue, a robotic arm (KINOVA, Gen2- 7 DOF) was implemented to hold the camera at a fixed location for both data collection and CF controller stages. The position of the camera was based on an electromagnetic(EM) tracker sensor(Polhemus vipe, 6DOF) that was attached to the catheter. The robotic arm was acting as the X-ray fluoroscopy machine in the real-world surgical operating room.

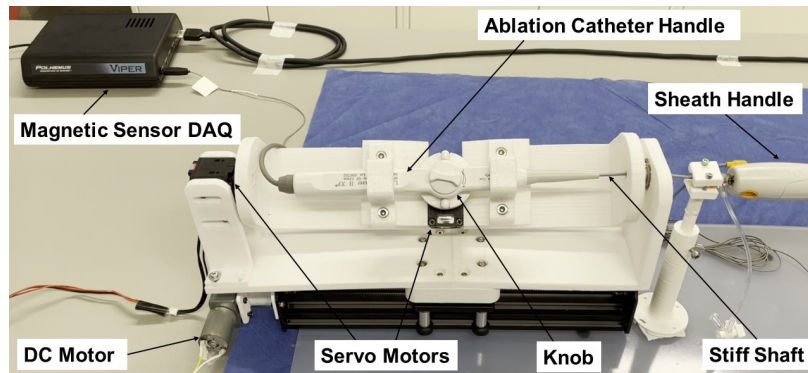
Finally, the CF controller platform consisting of a catheter manipulator, vision system, and heart-beating simulator was developed to evaluate the performance of the proposed controller schema.

Data collection for the model

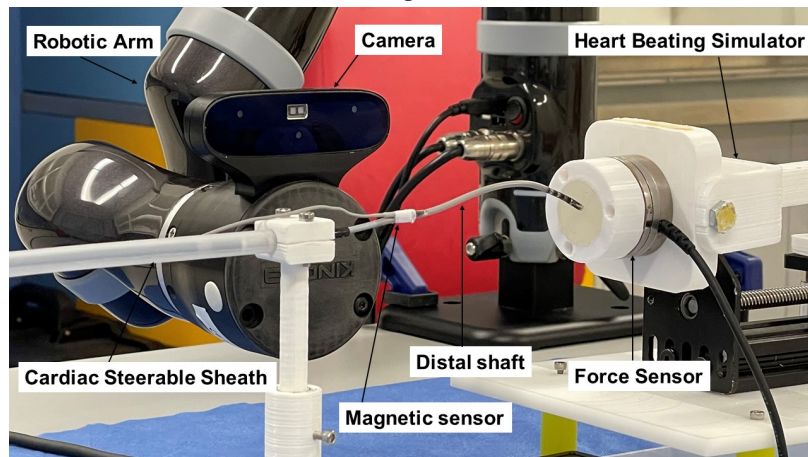
The process of data collection was similar to the previous paper of the author, Khodashenas. *et al.*[101]. As illustrated in Figure.4.5a, a stepper motor(17HS4401-S 40mm Nema) drives the linear actuator for a defined limit to push the catheter’s tip. The driver of the motor receives commands from a micro-controller(Arduino UNO) that is communicating with a computer program developed in Python. For every actuation of the mechanism, the image of the bending section of the distal shaft of the catheter and its corresponding forces were stored in the computer. This process was followed for 2000 samples to finally arrange the dataset consisting of images of the distal shaft from the initial



(a) Overall View



(b) Catheter Manipulator Mechanism



(c) Robotic Arm and bending section

Figure 4.5: Experimental setup

shape to fully curved one and also matched forces of each bending. To make sure that the camera maintains a fixed location and position to the bending section, the robotic arm was implemented. To adjust the relative position and distance of the camera with the bending section, an EM sensor was attached at the conjunction of the distal and stiff shaft of the catheter to be used for the robot's localization. After fixing the camera at the desired place, the relative geometrical values were stored to be used for the CF controller.

Vision system

As mentioned above, a robotic arm was used to stabilize the camera, meaning that the distal shaft is always in a fixed view of the camera. So, the dataset's images are valid for the CF controller system. If the robotic catheter manipulator rotates the catheter around its shaft, consequently the robotic end-effector moves relative to the rotation of the bending section plane. As the result, the camera and the bending section move simultaneously to provide a constant image of the distal shaft.

This system is capable of tracking the catheter from the start of insertion of the catheter from the human vein till the end of the ablation procedure. In fully or semi-robotic surgeries, because the proposed system locks on the target area, the robotic arm can be used for the detection of potential contacts of the catheter with veins.

Robotic mechanism for the controller

Figure.4.5b depicts the 3-DoF catheter manipulator mechanism developed for the CF control. The camera of the vision system captures images and sends them to the computer program developed in Python to be fed into the feature extraction algorithm and estimator. The control mechanism pushes an ablation catheter(Boston Scientific Blazer II XP) against a surface. This actuator was designed in SolidWorks 2020 and fabricated by a 3D printer(MakerBot - Replicator+). The catheter handle was attached to the mechanism and two servo motors (Dynamixel XL430-W250) were deployed for maneuvering the knob of the catheter and to rotate the handle around its shaft. A geared DC motor(5840-31ZY, 130 RPM) was connected to a linear actuator that moves the catheter forward and backward. The knob of the catheter is a rotary mechanism for bending the distal shaft by pulling tendons inside the catheter's shaft. In clinical application, this knob is used for steering

the catheter into the heart[13] and for applying the CF, the surgeon advances the catheter against the tissue. In this study, the knob was adjusted at the neutral position in which the distal shaft was not under the tendon's tension. The DC motor is powered by an H-bridge driver(DFROBOT 2X2A DC Motor Shield for Arduino) that receives commands from the computer program for moving the catheter to apply the desired CF. To simulate the sinusoidal beating of the heart, a linear actuator powered by a stepper motor oscillates against the catheter's tip.

4.3 Validation studies

In this section, to investigate the feasibility of the proposed system, the neural CF estimator performance has been evaluated. Also, two experimental validation tests were performed to examine the CF controller. The first test was intended to assess the controller functionality for constant input forces for a defined time interval. Following this experimental test, in order to investigate the fast response of the controller, desired forces were sinusoidal with two different frequencies.

4.3.1 CF estimator evaluation

The final model had a mean absolute error of 0.012 ± 0.01 with goodness-of-fit of $R^2 = 0.99$. Figure.4.6a depicts the training and validation loss for number of epochs and also the Figure.4.6b shows the correlation of actual and prediction values of CF(F_z). This optimal ANN model accurately estimates the CF for all potential bending of the distal shaft. A comparison of the actual and estimated force values of all data points in the dataset has been made and the results shows the accuracy of the neural force estimator(Figure.4.6d). Also in Figure.4.6c, the distribution of the error is demonstrated.

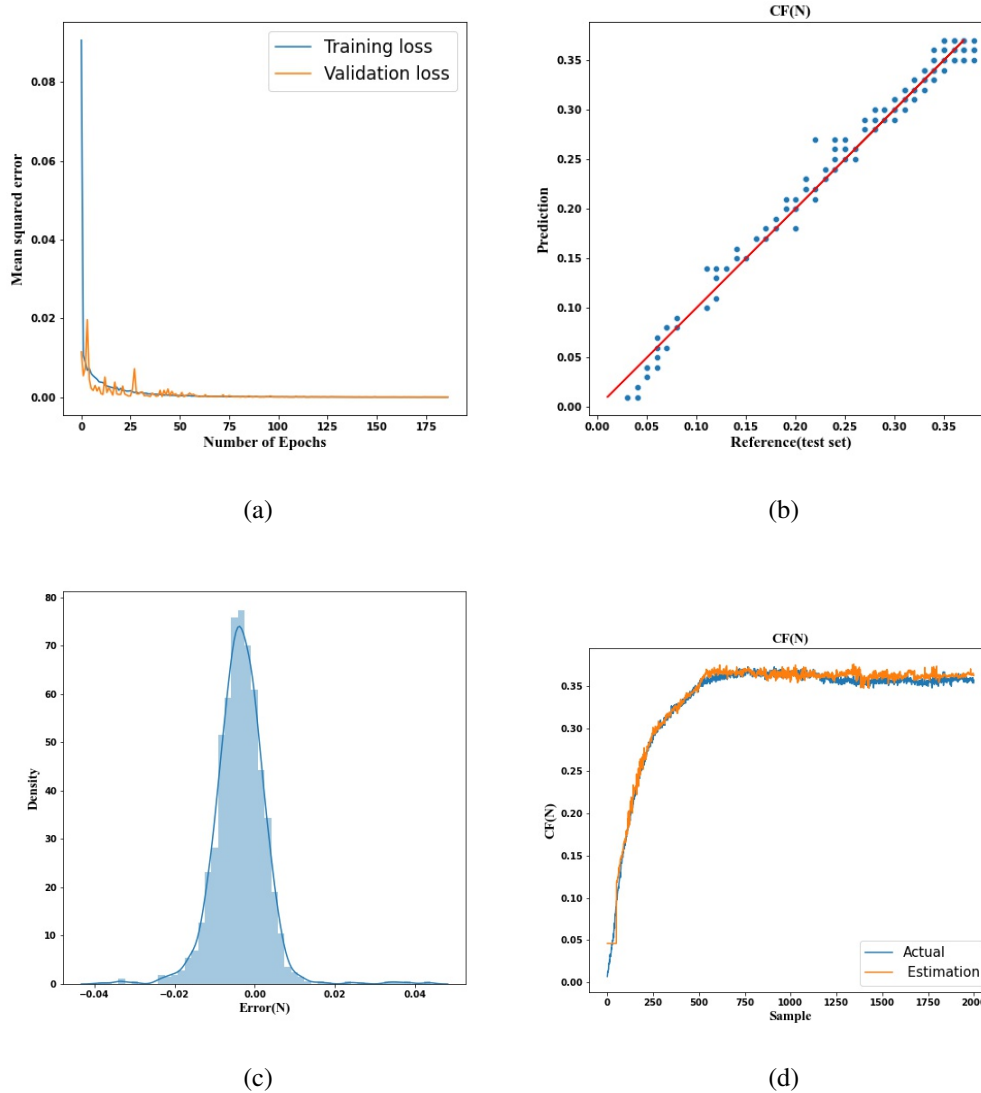


Figure 4.6: Model performance analysis - (a) Training loss diagram for validation and training set, (b) Correlation of the reference values from test set and the estimation of the model, (c) Error distribution, (d) Comparison of all actual and predicted CFs.

4.3.2 Static force control

The response of the controller was evaluated for a step input force of 0.2 (N) as shown in Figure.4.7. The results showed the 0.02 N overshoot and 0.2 second rise time. To test the system for constant desired forces, the input from 0.05 N to 0.3 N for 5 seconds interval was changed. As shown in Figure.4.8a, the controller followed the desired CF and the system illustrates an RMS

error of $0.01 \pm 0.01N$.

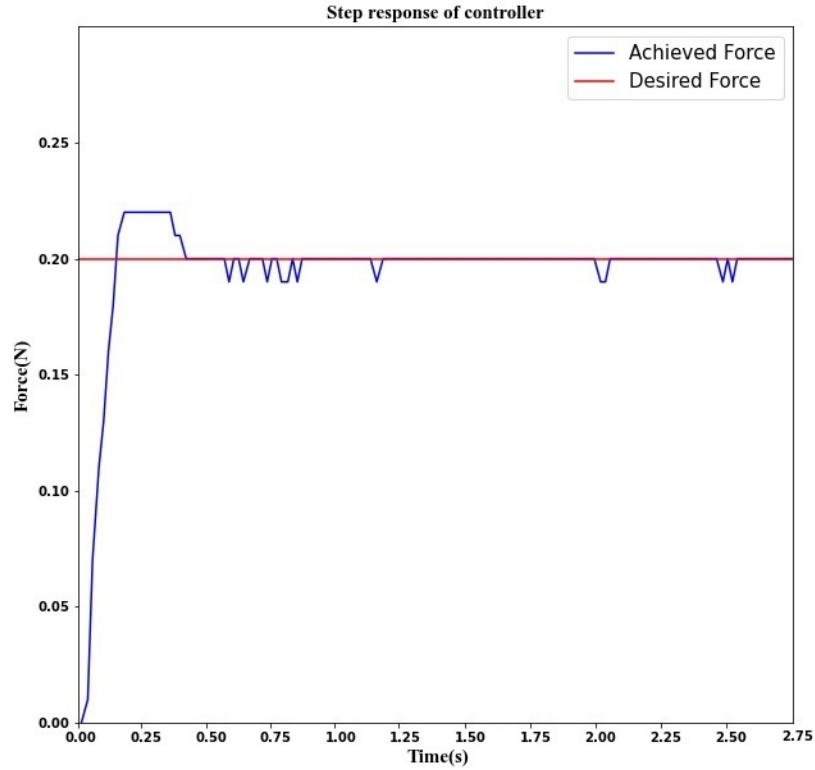
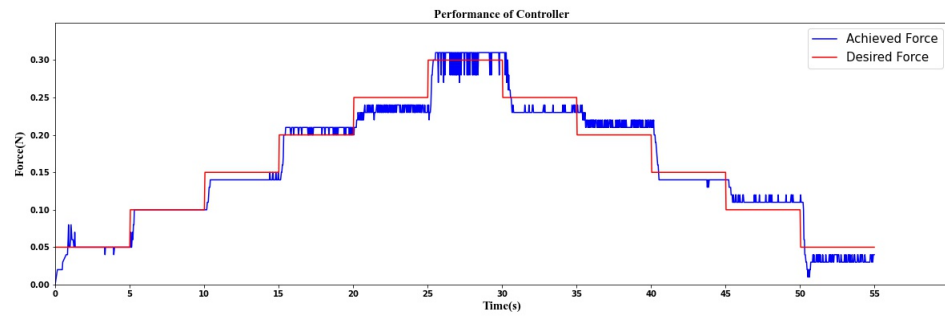


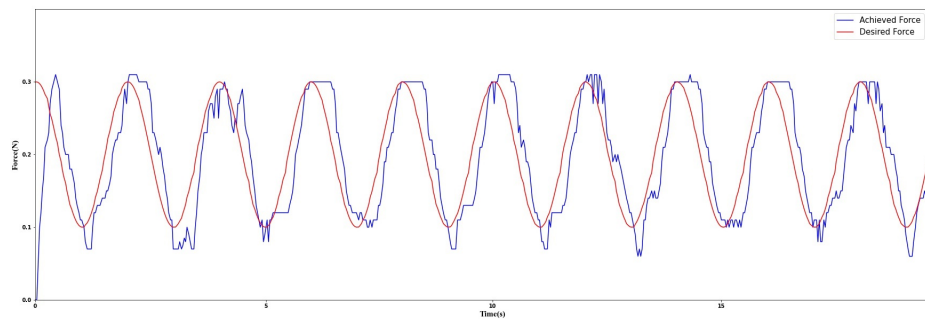
Figure 4.7: Step response analysis

4.3.3 Dynamic force control

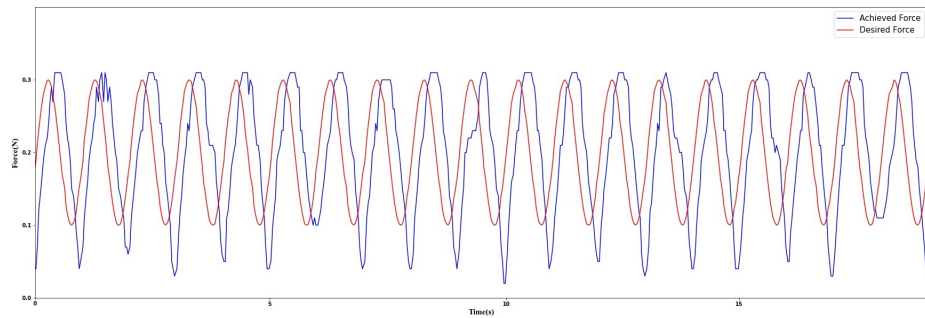
In this experimental evaluation, the desired input force was changed over time to test the functionality of the system for fast response. The desired forces were sinusoidal with peak-to-peak amplitude of $0.2 N$ and frequency of $0.5 Hz$ and $1 Hz$. Figure.4.8b compares the desired and achieved forces in $0.5 Hz$ mode. The system was capable of maintaining the force with an RMS-error of $0.04 \pm 0.03 N$ for $0.5 Hz$ test. Figure.4.8c shows the performance of the controller for $1 Hz$ input forces. For this test, he RMS-error was $0.06 \pm 0.03 N$.



(a)



(b)



(c)

Figure 4.8: Validation tests - (a) Static force input, (b) 0.5 Hz sinusoidal force input, (c) 1Hz sinusoidal force input

4.4 Conclusion

In this study, a sensor-less CF control system for ablation catheters was proposed and validated. A mechanical mechanism was designed to insert the catheter and achieve the desired CF by using a

visual feedback element. A robotic arm was deployed to mimic the X-ray fluoroscopy machine and to make sure that the camera is located at a fixed location. The controller feedback was a vision-based schema consisting of a feature extraction algorithm and a fully-coupled ANN to estimate the CF directly from the image of the camera. The proposed sensor-free controller was tested for constant and sinusoidal desired forces and as the result, the system fairly followed the desired CFs. In the present study, a standard ablation catheter was used for the test and it can be quickly attached to the designed mechanism for CF control.

One limitation of the system is the segmentation of the catheter through a binary threshold operation that can be more robust by using an object detection and segmentation algorithm to extract the catheter from the noisy background image. In addition, a position control schema can be added to the proposed system to guide the catheter's tip to the desired location and then apply the required CF.

Chapter 5

Conclusion and Future Works

5.1 Conclusions

Catheter ablation is known as the curative treatment of the choice for atrial fibrillation heart failure. The CF plays an important role in the success rate of the heart ablation procedure. Having a sense of touch for the surgeon during this minimally invasive surgery considerably increases the sustainability and efficacy of the surgery. Furthermore, robotic-assisted surgery enables surgeons to perform the surgery accurately and safely. The CF controller is a part of robotic systems for heart ablation surgery to maintain the catheter-tissue CF at the desired value. To apply adequate CF for the ablation procedure, a sensing method and also a controller schema are essential. To measure the applied force, methods fall into two categories including sensor-based and sensor-free. Due to limitations of sensor-based technologies such as design complications, cost, and measurement calibration, the sensor-free approach has demonstrated promising results. In this method, usually, the bending of a commercial standard catheter's shaft under applied forces is visually analyzed to estimate the CF. The accurate and fast estimator can be implemented as a feedback element in the CF controller to hold the CF at a required safe value. To this end, the objective of the present thesis was to design, evaluate and implement a real-time, accurate, and image-based CF controller for ablation therapy.

To address the aforementioned clinical need, an estimator based on machine learning algorithms

was introduced and validated to be used as the feedback element of the CF controller. In this thesis, firstly in an attempt to design an image-enabled estimator, experimental setups were designed and fabricated. The design principle and data acquisition process was described in Chapter 2. The aim of using the mentioned setups is to compile a dataset consisting of images of the catheter's bending under applied forces and corresponding forces. In the compiled dataset, just one camera normal to the bending section of the catheter(distal shaft) was deployed. As a result, the dataset was a combination of images and the applied CF from the external force sensor. After arranging the dataset and performing pre-processing operations, a feature extraction algorithm was deployed to use features for the training of machine learning models. The image-based feature extraction algorithm was introduced in Chapter 3 and different types of machine learning models such as artificial neural network and support vector regression were tested and validated. After Choosing the appropriate model capable of estimating the CF precisely and quickly, the estimator was implemented as a feedback element in a control loop.

The estimator of the choice successfully was used to provide the CF with a mean absolute error of $0.012 \pm 0.01 N$ which is less than 10% of the full-scale CF value($0 - 0.3 N$). In addition, the estimator demonstrated acceptable speed to be used in real-time control by taking less than 0.02 seconds per video frame. In continuation, the vision-based estimator was deployed as a feedback element in a PD control loop to maintain the CF at the desired value. A catheter manipulator mechanism was designed to apply the control signal by pushing the catheter against a surface that was described in Chapter 4. In an attempt to provide a constant image for the controller from the distal shaft of the catheter, a robotic arm was used that moves and rotates simultaneously with the catheter manipulator. This robotic imaging system was acting as the X-ray imaging system of the surgical operating room. The system was able to maintain the CF with root-mean-squared(RMS) error of $0.01 \pm 0.01 N$ for static test and RMS error of $0.04 \pm 0.03 N$ for dynamic input forces.

As the present research demonstrated, the vision-based estimator and controller were feasible, accurate, fast, and clinically realistic to estimate the CF just from the X-ray images of the ablation surgery and consequently control it. The system can be used as a part of a fully or semi-robotic surgery procedure in an attempt to improve the outcome of the surgery.

5.2 Future Works

The limitations of this research can be tackled to improve the proposed systems in future studies.

To address the improvements in the subsequent research:

- (1) The vision-based method introduced in Chapter 3 extracts features after a binary threshold operation as a preprocessing step. This image processing step can be improved by having an image segmentation algorithm capable of segmenting the catheter's distal shaft from the background of the image.
- (2) The control loop described in Chapter 4 is a PD controller that gains were tuned manually. The tuning process is time-consuming and also dependent on the design of the system. In this regard, an adaptive controller or auto-tuning methods such as genetic algorithms can be deployed to make sure the gains are tuned automatically and the system is robust.
- (3) The proposed CF controller can be improved by developing a position controller that manipulates the catheter's tip to the target spot. The designed catheter manipulator mechanism is capable of actuating the catheter in 3-DoF accurately, so this capability can make the system ideal for a hybrid position-force control.

Bibliography

- [1] S. S. Virani, A. Alonso, E. J. Benjamin, M. S. Bittencourt, C. W. Callaway, A. P. Carson, A. M. Chamberlain, A. R. Chang, S. Cheng, F. N. Delling, *et al.*, “Heart disease and stroke statistics—2020 update: a report from the american heart association,” *Circulation*, vol. 141, no. 9, pp. e139–e596, 2020.
- [2] Centers for Disease Control and Prevention (CDC), “Heart disease facts.” <https://www.cdc.gov/heartdisease/facts.htm>. Accessed: 2022-11-01.
- [3] S. S. Virani, A. Alonso, H. J. Aparicio, E. J. Benjamin, M. S. Bittencourt, C. W. Callaway, A. P. Carson, A. M. Chamberlain, S. Cheng, F. N. Delling, *et al.*, “Heart disease and stroke statistics—2021 update: a report from the american heart association,” *Circulation*, vol. 143, no. 8, pp. e254–e743, 2021.
- [4] P. Bittihn, *Complex structure and dynamics of the heart*. Springer, 2014.
- [5] S. Nattel, “New ideas about atrial fibrillation 50 years on,” *Nature*, vol. 415, no. 6868, pp. 219–226, 2002.
- [6] J. Kornej, C. S. Börschel, E. J. Benjamin, and R. B. Schnabel, “Epidemiology of atrial fibrillation in the 21st century: novel methods and new insights,” *Circulation research*, vol. 127, no. 1, pp. 4–20, 2020.
- [7] C. Basso, D. Corrado, F. I. Marcus, A. Nava, and G. Thiene, “Arrhythmogenic right ventricular cardiomyopathy,” *The Lancet*, vol. 373, no. 9671, pp. 1289–1300, 2009.

- [8] E. N. Prystowsky, B. J. Padanilam, and R. I. Fogel, "Treatment of atrial fibrillation," *Jama*, vol. 314, no. 3, pp. 278–288, 2015.
- [9] O. M. Wazni, N. F. Marrouche, D. O. Martin, A. Verma, M. Bhargava, W. Saliba, D. Bash, R. Schweikert, J. Brachmann, J. Gunther, *et al.*, "Radiofrequency ablation vs antiarrhythmic drugs as first-line treatment of symptomatic atrial fibrillation: a randomized trial," *Jama*, vol. 293, no. 21, pp. 2634–2640, 2005.
- [10] N. Bandari, J. Dargahi, and M. Packirisamy, "Tactile sensors for minimally invasive surgery: A review of the state-of-the-art, applications, and perspectives," *Ieee Access*, vol. 8, pp. 7682–7708, 2019.
- [11] G. Ndrepepa and H. Estner, "Ablation of cardiac arrhythmias—energy sources and mechanisms of lesion formation," in *Catheter Ablation of Cardiac Arrhythmias*, pp. 35–53, Springer, 2006.
- [12] D. Haemmerich, "Biophysics of radiofrequency ablation," *Critical Reviews™ in Biomedical Engineering*, vol. 38, no. 1, 2010.
- [13] X. Hu, A. Chen, Y. Luo, C. Zhang, and E. Zhang, "Steerable catheters for minimally invasive surgery: a review and future directions," *Computer Assisted Surgery*, vol. 23, no. 1, pp. 21–41, 2018.
- [14] M. Haissaguerre, L. Gencel, B. Fischer, P. Le Metayer, F. Poquet, F. I. Marcus, and J. Clementy, "Successful catheter ablation of atrial fibrillation," *Journal of cardiovascular electrophysiology*, vol. 5, no. 12, pp. 1045–1052, 1994.
- [15] K. Hirao, ed., *Catheter Ablation*. Singapore: Springer Singapore, 2018.
- [16] S. Neadios, P. Sommer, A. Bollmann, and G. Hindricks, "Advanced mapping systems to guide atrial fibrillation ablation: electrical information that matters," *Journal of atrial fibrillation*, vol. 8, no. 6, 2016.

- [17] R. Hofstetter, M. Slomczykowski, M. Sati, and L.-P. Nolte, "Fluoroscopy as an imaging means for computer-assisted surgical navigation," *Computer Aided Surgery*, vol. 4, no. 2, pp. 65–76, 1999.
- [18] H. Calkins, L. Niklason, J. Sousa, R. El-Atassi, J. Langberg, and F. Morady, "Radiation exposure during radiofrequency catheter ablation of accessory atrioventricular connections.," *Circulation*, vol. 84, no. 6, pp. 2376–2382, 1991.
- [19] A. Hooshiar, S. Najarian, and J. Dargahi, "Haptic telerobotic cardiovascular intervention: a review of approaches, methods, and future perspectives," *IEEE reviews in biomedical engineering*, vol. 13, pp. 32–50, 2019.
- [20] A. R. Lanfranco, A. E. Castellanos, J. P. Desai, and W. C. Meyers, "Robotic surgery: a current perspective," *Annals of surgery*, vol. 239, no. 1, p. 14, 2004.
- [21] F. R. y Baena and B. Davies, "Robotic surgery: from autonomous systems to intelligent tools," *Robotica*, vol. 28, no. 2, pp. 163–170, 2010.
- [22] M. J. Mack, "Minimally invasive and robotic surgery," *Jama*, vol. 285, no. 5, pp. 568–572, 2001.
- [23] J. K. Mullins, M. S. Borofsky, M. E. Allaf, S. Bhayani, J. H. Kaouk, C. G. Rogers, S. P. Hillyer, B. F. Kaczmarek, Y. S. Tanagho, and M. D. Stifelman, "Live robotic surgery: are outcomes compromised?," *Urology*, vol. 80, no. 3, pp. 602–607, 2012.
- [24] A. Tewari, J. Peabody, R. Sarle, G. Balakrishnan, A. Hemal, A. Shrivastava, and M. Menon, "Technique of da vinci robot-assisted anatomic radical prostatectomy," *Urology*, vol. 60, no. 4, pp. 569–572, 2002.
- [25] J. Reisenauer, M. J. Simoff, M. A. Pritchett, D. E. Ost, A. Majid, C. Keyes, R. F. Casal, M. S. Parikh, J. Diaz-Mendoza, S. Fernandez-Bussy, *et al.*, "Ion: technology and techniques for shape-sensing robotic-assisted bronchoscopy," *The Annals of thoracic surgery*, vol. 113, no. 1, pp. 308–315, 2022.

- [26] R. Tarwala and L. D. Dorr, “Robotic assisted total hip arthroplasty using the mako platform,” *Current reviews in musculoskeletal medicine*, vol. 4, no. 3, pp. 151–156, 2011.
- [27] M. Roche, “The mako robotic-arm knee arthroplasty system,” *Archives of Orthopaedic and Trauma Surgery*, vol. 141, no. 12, pp. 2043–2047, 2021.
- [28] A. Harky, G. Chaplin, J. S. K. Chan, P. Eriksen, B. MacCarthy-Ofosu, T. Theologou, and A. D. Muir, “The future of open heart surgery in the era of robotic and minimal surgical interventions,” *Heart, Lung and Circulation*, vol. 29, no. 1, pp. 49–61, 2020.
- [29] R. Bai, L. Di Biase, M. Valderrabano, F. Lorgat, H. Mlcochova, R. Tilz, U. Meyerfeldt, P. M. Hranitzky, O. Wazni, P. Kanagaratnam, *et al.*, “Worldwide experience with the robotic navigation system in catheter ablation of atrial fibrillation: methodology, efficacy and safety,” *Journal of cardiovascular electrophysiology*, vol. 23, no. 8, pp. 820–826, 2012.
- [30] B. Schmidt, K. R. J. Chun, R. R. Tilz, B. Koektuerk, F. Ouyang, and K.-H. Kuck, “Remote navigation systems in electrophysiology,” *Europace*, vol. 10, no. suppl_3, pp. iii57–iii61, 2008.
- [31] P. Aagaard, A. Natale, and L. Di Biase, “Robotic navigation for catheter ablation: benefits and challenges,” *Expert review of medical devices*, vol. 12, no. 4, pp. 457–469, 2015.
- [32] J. Bonatti, G. Vetrovec, C. Riga, O. Wazni, and P. Stadler, “Robotic technology in cardiovascular medicine,” *Nature Reviews Cardiology*, vol. 11, no. 5, pp. 266–275, 2014.
- [33] L. Di Biase, Y. Wang, R. Horton, G. J. Gallinghouse, P. Mohanty, J. Sanchez, D. Patel, M. Dare, R. Canby, L. D. Price, *et al.*, “Ablation of atrial fibrillation utilizing robotic catheter navigation in comparison to manual navigation and ablation: Single-center experience,” *Journal of cardiovascular electrophysiology*, vol. 20, no. 12, pp. 1328–1335, 2009.
- [34] G. A. Antoniou, C. V. Riga, E. K. Mayer, N. J. Cheshire, and C. D. Bicknell, “Clinical applications of robotic technology in vascular and endovascular surgery,” *Journal of vascular surgery*, vol. 53, no. 2, pp. 493–499, 2011.

- [35] M. Shurrab, R. Schilling, E. Gang, E. M. Khan, and E. Crystal, “Robotics in invasive cardiac electrophysiology,” *Expert review of medical devices*, vol. 11, no. 4, pp. 375–381, 2014.
- [36] Z. A. Shaikh, M. F. Eilenberg, and T. J. Cohen, “The amigo™ remote catheter system: from concept to bedside,” *The Journal of Innovations in Cardiac Rhythm Management*, vol. 8, no. 8, p. 2795, 2017.
- [37] A. Tolga, S. Bozyel, E. Golcuk, K. Yalin, and T. E. Guler, “Atrial fibrillation ablation using magnetic navigation comparison with conventional approach during long-term follow-up,” *Journal of Atrial Fibrillation*, vol. 8, no. 3, 2015.
- [38] D. Haines, “Biophysics of ablation: application to technology,” *Journal of cardiovascular electrophysiology*, vol. 15, pp. S2–S11, 2004.
- [39] N. Ariyaratna, S. Kumar, S. P. Thomas, W. G. Stevenson, and G. F. Michaud, “Role of contact force sensing in catheter ablation of cardiac arrhythmias: evolution or history repeating itself?,” *Clinical Electrophysiology*, vol. 4, no. 6, pp. 707–723, 2018.
- [40] C.-F. Tsai, C.-T. Tai, W.-C. Yu, Y.-J. Chen, M.-H. Hsieh, C.-E. Chiang, Y.-A. Ding, M.-S. Chang, and S.-A. Chen, “Is 8-mm more effective than 4-mm tip electrode catheter for ablation of typical atrial flutter?,” *Circulation*, vol. 100, no. 7, pp. 768–771, 1999.
- [41] H. Nakagawa, W. S. Yamanashi, J. V. Pitha, M. Arruda, X. Wang, K. Ohtomo, K. J. Beckman, J. H. McClelland, R. Lazzara, and W. M. Jackman, “Comparison of in vivo tissue temperature profile and lesion geometry for radiofrequency ablation with a saline-irrigated electrode versus temperature control in a canine thigh muscle preparation,” *Circulation*, vol. 91, no. 8, pp. 2264–2273, 1995.
- [42] L. Di Biase, A. Natale, C. Barrett, C. Tan, C. S. Elayi, C. K. Ching, P. Wang, A. AL-AHMAD, M. Arruda, J. D. Burkhardt, *et al.*, “Relationship between catheter forces, lesion characteristics, “popping,” and char formation: experience with robotic navigation system,” *Journal of cardiovascular electrophysiology*, vol. 20, no. 4, pp. 436–440, 2009.

- [43] M. Shurrab, L. Di Biase, D. F. Briceno, A. Kaoutskaia, S. Haj-Yahia, D. Newman, I. Lashovsky, H. Nakagawa, and E. Crystal, “Impact of contact force technology on atrial fibrillation ablation: a meta-analysis,” *Journal of the American Heart Association*, vol. 4, no. 9, p. e002476, 2015.
- [44] D. E. Haines, “Determinants of lesion size during radiofrequency catheter ablation: The role of electrode-tissue contact pressure and duration of energy delivery,” *Journal of cardiovascular electrophysiology*, vol. 2, no. 6, pp. 509–515, 1991.
- [45] A. Thiagalingam, A. D’AVILA, L. Foley, J. L. Guerrero, H. Lambert, G. Leo, J. N. Ruskin, and V. Y. Reddy, “Importance of catheter contact force during irrigated radiofrequency ablation: evaluation in a porcine ex vivo model using a force-sensing catheter,” *Journal of cardiovascular electrophysiology*, vol. 21, no. 7, pp. 806–811, 2010.
- [46] D. C. Shah and M. Namdar, “Real-time contact force measurement: a key parameter for controlling lesion creation with radiofrequency energy,” *Circulation: Arrhythmia and Electrophysiology*, vol. 8, no. 3, pp. 713–721, 2015.
- [47] K. Xu and N. Simaan, “An investigation of the intrinsic force sensing capabilities of continuum robots,” *IEEE Transactions on Robotics*, vol. 24, no. 3, pp. 576–587, 2008.
- [48] P. French, D. Tanase, and J. Goosen, “Sensors for catheter applications,” *Sensors Update*, vol. 13, no. 1, pp. 107–153, 2003.
- [49] L. Zou, C. Ge, Z. J. Wang, E. Cretu, and X. Li, “Novel tactile sensor technology and smart tactile sensing systems: A review,” *Sensors*, vol. 17, no. 11, p. 2653, 2017.
- [50] V. Y. Reddy, S. R. Dukkupati, P. Neuzil, A. Natale, J.-P. Albenque, J. Kautzner, D. Shah, G. Michaud, M. Wharton, D. Harari, *et al.*, “Randomized, controlled trial of the safety and effectiveness of a contact force-sensing irrigated catheter for ablation of paroxysmal atrial fibrillation: results of the tacticath contact force ablation catheter study for atrial fibrillation (toccstar) study,” *Circulation*, vol. 132, no. 10, pp. 907–915, 2015.

- [51] G. Lee, R. J. Hunter, M. J. Lovell, M. Finlay, W. Ullah, V. Baker, M. B. Dhinoja, S. Sporton, M. J. Earley, and R. J. Schilling, "Use of a contact force-sensing ablation catheter with advanced catheter location significantly reduces fluoroscopy time and radiation dose in catheter ablation of atrial fibrillation," *EP Europace*, vol. 18, no. 2, pp. 211–218, 2016.
- [52] K. Yokoyama, H. Nakagawa, D. C. Shah, H. Lambert, G. Leo, N. Aeby, A. Ikeda, J. V. Pitha, T. Sharma, R. Lazzara, *et al.*, "Novel contact force sensor incorporated in irrigated radiofrequency ablation catheter predicts lesion size and incidence of steam pop and thrombus," *Circulation: Arrhythmia and Electrophysiology*, vol. 1, no. 5, pp. 354–362, 2008.
- [53] M. Borlich, L. Iden, K. Kuhnhardt, I. Paetsch, G. Hindricks, and P. Sommer, "3d mapping for pvi-geometry, image integration and incorporation of contact force into work flow," *Journal of atrial fibrillation*, vol. 10, no. 6, 2018.
- [54] T. Lin, F. Ouyang, K.-H. Kuck, and R. Tilz, "Thermocool® smarttouch® catheter—the evidence so far for contact force technology and the role of visitag™ module," *Arrhythmia & electrophysiology review*, vol. 3, no. 1, p. 44, 2014.
- [55] C. A. Martin, R. Martin, P. R. Gajendragadkar, P. Maury, M. Takigawa, G. Cheniti, A. Frontera, T. Kitamura, J. Duchateau, K. Vlachos, *et al.*, "First clinical use of novel ablation catheter incorporating local impedance data," *Journal of Cardiovascular Electrophysiology*, vol. 29, no. 9, pp. 1197–1206, 2018.
- [56] S. Guo, M. Qin, N. Xiao, Y. Wang, W. Peng, and X. Bao, "High precise haptic device for the robotic catheter navigation system," in *2016 IEEE International Conference on Mechatronics and Automation*, pp. 2524–2529, IEEE, 2016.
- [57] G. Robinson and J. B. C. Davies, "Continuum robots-a state of the art," in *Proceedings 1999 IEEE international conference on robotics and automation (Cat. No. 99CH36288C)*, vol. 4, pp. 2849–2854, IEEE, 1999.
- [58] Y. Bailly and Y. Amirat, "Modeling and control of a hybrid continuum active catheter for aortic aneurysm treatment," in *Proceedings of the 2005 IEEE international conference on robotics and automation*, pp. 924–929, IEEE, 2005.

- [59] D. B. Camarillo, C. F. Milne, C. R. Carlson, M. R. Zinn, and J. K. Salisbury, "Mechanics modeling of tendon-driven continuum manipulators," *IEEE transactions on robotics*, vol. 24, no. 6, pp. 1262–1273, 2008.
- [60] M. Khoshnam, M. Azizian, and R. V. Patel, "Modeling of a steerable catheter based on beam theory," in *2012 IEEE International Conference on Robotics and Automation*, pp. 4681–4686, IEEE, 2012.
- [61] M. Khoshnam and R. V. Patel, "Estimating contact force for steerable ablation catheters based on shape analysis," in *2014 IEEE/RSJ International Conference on Intelligent Robots and Systems*, pp. 3509–3514, IEEE, 2014.
- [62] M. Khoshnam, A. Yurkewich, and R. V. Patel, "Model-based force control of a steerable ablation catheter with a custom-designed strain sensor," in *2013 IEEE International Conference on Robotics and Automation*, pp. 4479–4484, IEEE, 2013.
- [63] A. A. Shabana, "Flexible multibody dynamics: review of past and recent developments," *Multibody system dynamics*, vol. 1, no. 2, pp. 189–222, 1997.
- [64] P. Flores and H. M. Lankarani, *Contact force models for multibody dynamics*, vol. 226. Springer, 2016.
- [65] T. Alderliesten, M. K. Konings, and W. J. Niessen, "Simulation of minimally invasive vascular interventions for training purposes," *Computer Aided Surgery*, vol. 9, no. 1-2, pp. 3–15, 2004.
- [66] W. Tang, T. R. Wan, D. A. Gould, T. How, and N. W. John, "A stable and real-time nonlinear elastic approach to simulating guidewire and catheter insertions based on cosserat rod," *IEEE Transactions on Biomedical Engineering*, vol. 59, no. 8, pp. 2211–2218, 2012.
- [67] A. Hooshidar, A. Sayadi, M. Jolaei, and J. Dargahi, "Analytical tip force estimation on tendon-driven catheters through inverse solution of cosserat rod model," in *2021 IEEE/RSJ International Conference on Intelligent Robots and Systems (IROS)*, pp. 1829–1834, IEEE, 2021.

- [68] J. Lenoir, S. Cotin, C. Duriez, and P. Neumann, “Interactive physically-based simulation of catheter and guidewire,” *Computers & Graphics*, vol. 30, no. 3, pp. 416–422, 2006.
- [69] S. Hasanzadeh and F. Janabi-Sharifi, “Model-based force estimation for intracardiac catheters,” *IEEE/ASME Transactions on Mechatronics*, vol. 21, no. 1, pp. 154–162, 2015.
- [70] G. Runge, M. Wiese, and A. Raatz, “Fem-based training of artificial neural networks for modular soft robots,” in *2017 IEEE International Conference on Robotics and Biomimetics (ROBIO)*, pp. 385–392, IEEE, 2017.
- [71] M. Jolaei, A. Hooshier, J. Dargahi, and M. Packirisamy, “Toward task autonomy in robotic cardiac ablation: Learning-based kinematic control of soft tendon-driven catheters,” *Soft Robotics*, vol. 8, no. 3, pp. 340–351, 2021.
- [72] A. Hooshier, A. Sayadi, J. Dargahi, and S. Najarian, “Integral-free spatial orientation estimation method and wearable rotation measurement device for robot-assisted catheter intervention,” *IEEE/ASME Transactions on Mechatronics*, vol. 27, no. 2, pp. 766–776, 2021.
- [73] A. Sayadi, H. R. Nourani, M. Jolaei, J. Dargahi, and A. Hooshier, “Force estimation on steerable catheters through learning-from-simulation with ex-vivo validation,” in *2021 International Symposium on Medical Robotics (ISMR)*, pp. 1–6, IEEE, 2021.
- [74] H. Nourani, *imaged-based tip force estimation on steerable intracardiac catheters using learning-based methods*. PhD thesis, Concordia University, 2021.
- [75] F. Feng, W. Hong, and L. Xie, “A learning-based tip contact force estimation method for tendon-driven continuum manipulator,” *Scientific Reports*, vol. 11, no. 1, pp. 1–11, 2021.
- [76] J. Back, T. Manwell, R. Karim, K. Rhode, K. Althoefer, and H. Liu, “Catheter contact force estimation from shape detection using a real-time cosserat rod model,” in *2015 IEEE/RSJ International Conference on Intelligent Robots and Systems (IROS)*, pp. 2037–2042, IEEE, 2015.

- [77] J. Back, L. Lindenroth, K. Rhode, and H. Liu, “Three dimensional force estimation for steerable catheters through bi-point tracking,” *Sensors and Actuators A: Physical*, vol. 279, pp. 404–415, 2018.
- [78] M. Kouh Soltani, S. Khanmohammadi, and F. Ghalichi, “A three-dimensional shape-based force and stiffness-sensing platform for tendon-driven catheters,” *Sensors*, vol. 16, no. 7, p. 990, 2016.
- [79] P. Fekri, H. Khodashenas, K. Lachapelle, R. Cecere, M. Zadeh, and J. Dargahi, “Y-net: A deep convolutional architecture for 3d estimation of contact forces in intracardiac catheters,” *IEEE Robotics and Automation Letters*, vol. 7, no. 2, pp. 3592–3599, 2022.
- [80] World Health Organization (WHO), “Cardiovascular diseases.” https://www.who.int/health-topics/cardiovascular-diseases#tab=tab_1. *Accessed* : 2022 – 11 – 01.
- [81] P. B. Nery, R. Thornhill, G. M. Nair, E. Pena, and C. J. Redpath, “Scar-based catheter ablation for persistent atrial fibrillation,” *Current opinion in cardiology*, vol. 32, no. 1, pp. 1–9, 2017.
- [82] S. De Buck, J. Ector, A. La Gerche, F. Maes, and H. Heidbuchel, “Toward image-based catheter tip tracking for treatment of atrial fibrillation,” in *CI2BM09-MICCAI Workshop on Cardiovascular Interventional Imaging and Biophysical Modelling*, pp. 8–pages, 2009.
- [83] J. Till, V. Aloï, and C. Rucker, “Real-time dynamics of soft and continuum robots based on cosserat rod models,” *The International Journal of Robotics Research*, vol. 38, no. 6, pp. 723–746, 2019.
- [84] R. J. Webster III, J. M. Romano, and N. J. Cowan, “Mechanics of precurved-tube continuum robots,” *IEEE Transactions on Robotics*, vol. 25, no. 1, pp. 67–78, 2008.
- [85] I. Goodfellow, Y. Bengio, and A. Courville, *Deep Learning*. MIT Press, 2016. <http://www.deeplearningbook.org>.
- [86] M. Awad and R. Khanna, *Support Vector Regression*, pp. 67–80. Berkeley, CA: Apress, 2015.

- [87] N. Srivastava, G. Hinton, A. Krizhevsky, I. Sutskever, and R. Salakhutdinov, “Dropout: A simple way to prevent neural networks from overfitting,” *Journal of Machine Learning Research*, vol. 15, no. 56, pp. 1929–1958, 2014.
- [88] S. Ioffe and C. Szegedy, “Batch normalization: Accelerating deep network training by reducing internal covariate shift,” 2015.
- [89] D. P. Kingma and J. Ba, “Adam: A method for stochastic optimization,” 2017.
- [90] M. Abadi, A. Agarwal, P. Barham, E. Brevdo, Z. Chen, C. Citro, G. S. Corrado, A. Davis, J. Dean, M. Devin, S. Ghemawat, I. Goodfellow, A. Harp, G. Irving, M. Isard, Y. Jia, R. Jozefowicz, L. Kaiser, M. Kudlur, J. Levenberg, D. Mané, R. Monga, S. Moore, D. Murray, C. Olah, M. Schuster, J. Shlens, B. Steiner, I. Sutskever, K. Talwar, P. Tucker, V. Vanhoucke, V. Vasudevan, F. Viégas, O. Vinyals, P. Warden, M. Wattenberg, M. Wicke, Y. Yu, and X. Zheng, “TensorFlow: Large-scale machine learning on heterogeneous systems,” 2015. Software available from tensorflow.org.
- [91] F. Pedregosa, G. Varoquaux, A. Gramfort, V. Michel, B. Thirion, O. Grisel, M. Blondel, P. Prettenhofer, R. Weiss, V. Dubourg, J. Vanderplas, A. Passos, D. Cournapeau, M. Brucher, M. Perrot, and E. Duchesnay, “Scikit-learn: Machine learning in Python,” *Journal of Machine Learning Research*, vol. 12, pp. 2825–2830, 2011.
- [92] M. Wright, M. Haissaguerre, S. Knecht, S. Matsuo, M. D. O’NEILL, I. Nault, N. Lellouche, M. Hocini, F. Sacher, and P. Jais, “State of the art: catheter ablation of atrial fibrillation,” *Journal of cardiovascular electrophysiology*, vol. 19, no. 6, pp. 583–592, 2008.
- [93] S. D. Barnett and N. Ad, “Surgical ablation as treatment for the elimination of atrial fibrillation: a meta-analysis,” *The Journal of thoracic and cardiovascular surgery*, vol. 131, no. 5, pp. 1029–1035, 2006.
- [94] H. Nakagawa and W. M. Jackman, “The role of contact force in atrial fibrillation ablation,” *Journal of atrial fibrillation*, vol. 7, no. 1, 2014.

- [95] N. M. Bandari, R. Ahmadi, A. Hooshlar, J. Dargahi, and M. Packirisamy, “Hybrid piezoresistive-optical tactile sensor for simultaneous measurement of tissue stiffness and detection of tissue discontinuity in robot-assisted minimally invasive surgery,” *Journal of biomedical optics*, vol. 22, no. 7, p. 077002, 2017.
- [96] A. Sayadi, *Modeling and Force Estimation of Cardiac Catheters for Haptics-enabled Tele-intervention*. PhD thesis, Concordia University, 2021.
- [97] A. Hooshlar, A. Sayadi, M. Jolaei, and J. Dargahi, “Accurate estimation of tip force on tendon-driven catheters using inverse cosserat rod model,” in *2020 International Conference on Biomedical Innovations and Applications (BIA)*, pp. 37–40, IEEE, 2020.
- [98] M. R. Afzal, J. Chatta, A. Samanta, S. Waheed, M. Mahmoudi, R. Vukas, S. Gunda, M. Reddy, B. Dawn, and D. Lakkireddy, “Use of contact force sensing technology during radiofrequency ablation reduces recurrence of atrial fibrillation: a systematic review and meta-analysis,” *Heart Rhythm*, vol. 12, no. 9, pp. 1990–1996, 2015.
- [99] W. Ullah, R. J. Hunter, V. Baker, M. B. Dhinoja, S. Sporton, M. J. Earley, and R. J. Schilling, “Target indices for clinical ablation in atrial fibrillation: insights from contact force, electrogram, and biophysical parameter analysis,” *Circulation: Arrhythmia and Electrophysiology*, vol. 7, no. 1, pp. 63–68, 2014.
- [100] S. McFadden, R. Mooney, and P. Shepherd, “X-ray dose and associated risks from radiofrequency catheter ablation procedures,” *The British journal of radiology*, vol. 75, no. 891, pp. 253–265, 2002.
- [101] H. Khodashenas, P. Fekri, M. Zadeh, and J. Dargahi, “A vision-based method for estimating contact forces in intracardiac catheters,” in *2021 IEEE International Conference on Autonomous Systems (ICAS)*, pp. 1–7, IEEE, 2021.
- [102] S. B. Kesner and R. D. Howe, “Force control of flexible catheter robots for beating heart surgery,” in *2011 IEEE international conference on robotics and automation*, pp. 1589–1594, IEEE, 2011.

- [103] N. Kumar, J. Wirekoh, S. Saba, C. N. Riviere, and Y.-L. Park, “Soft miniaturized actuation and sensing units for dynamic force control of cardiac ablation catheters,” *Soft robotics*, vol. 8, no. 1, pp. 59–70, 2021.
- [104] D. Gelman, A. C. Skanes, M. A. Tavallaei, and M. Drangova, “Design and evaluation of a catheter contact-force controller for cardiac ablation therapy,” *IEEE Transactions on Biomedical Engineering*, vol. 63, no. 11, pp. 2301–2307, 2016.
- [105] M. Jolaei, A. Hooshir, A. Sayadi, J. Dargahi, and M. Packirisamy, “Sensor-free force control of tendon-driven ablation catheters through position control and contact modeling,” in *2020 42nd Annual International Conference of the IEEE Engineering in Medicine & Biology Society (EMBC)*, pp. 5248–5251, IEEE, 2020.